Citation: Molecular Therapy — Methods & Clinical Development (2015) **2,** 15003; doi:10.1038/mtm.2015.3

www.nature.com/mtm

ARTICLE

Nuclear expression of mitochondrial *ND4* leads to the protein assembling in complex I and prevents optic atrophy and visual loss

Hélène Cwerman-Thibault[1–3], Sébastien Augustin[1–3], Christophe Lechauve[1–3], Jessica Ayache[1–3], Sami Ellouze[1–3], José-Alain Sahel[1–3] and Marisol Corral-Debrinski[1–4]

Leber hereditary optic neuropathy is due to mitochondrial DNA mutations; in ~70% of all cases, a point mutation in the mitochondrial NADH dehydrogenase subunit 4, *ND4*, gene leads to central vision loss. We optimized allotopic expression (nuclear transcription of a gene that is normally transcribed inside the mitochondria) aimed at designing a gene therapy for *ND4*; its coding sequence was associated with the *cis*-acting elements of the human *COX10* mRNA to allow the efficient mitochondrial delivery of the protein. After ocular administration to adult rats of a recombinant adeno-associated viral vector containing the human *ND4* gene, we demonstrated that: (i) the sustained expression of human ND4 did not lead to harmful effects, instead the human protein is efficiently imported inside the mitochondria and assembled in respiratory chain complex I; (ii) the presence of the human protein in the experimental model of Leber hereditary optic neuropathy significantly prevents retinal ganglion cell degeneration and preserves both complex I function in optic nerves and visual function. Hence, the use of optimized allotopic expression is relevant for treating mitochondrial disorders due to mutations in the organelle genome.

Molecular Therapy — Methods & Clinical Development (2015) **2**, 15003; doi:10.1038/mtm.2015.3; published online 25 February 2015

INTRODUCTION

Leber hereditary optic neuropathy (LHON, MIM535000) is the most common illness caused by mitochondrial DNA (mtDNA) mutations, with an estimated prevalence of 1 in 40,000 in Europe.[1] In 95% of LHON cases, the disease is due to point mutations in the *ND1* (G3460A), *ND4* (G11778A), or *ND6* (T14484C) genes which encode proteins of the respiratory chain complex I (CI); about 70% of patients harbor the *ND4* mutation.[2] CI defect is the direct cause of retinal ganglion cell (RGC) loss and optic atrophy.[3] There is currently no treatment for LHON; even though recent reports described that idebenone (an analog of Coenzyme Q10) or EPI-743 (a para-benzoquinone) administration partially ameliorate the visual outcome of LHON patients.[4–6] LHON offers a unique opportunity for gene therapy setting for three reasons: (i) vision loss often occurs in a bilateral sequential fashion, the second eye becoming involved after the first with a median delay of 2 months,[7] thus, a prospect exists for a therapeutic intervention after vision loss in the first eye before second eye involvement; (ii) drugs or gene therapy vectors may be easily and directly delivered to RGCs, by injection into the vitreous body.[7,8] Thus, we intended to develop a strategy which could be translated to clinic research for LHON. Though, the techniques required for introducing genes directly into mitochondria are scarce yet, consequently, direct targeted repair or replacement of mutated mtDNA genes is not easy to perform except in yeast using biolistics strategies.[9] Progress could be obtained with the use of modified AAV vectors which could deliver DNA to the organelle as recently reported.[10,11] We choose to circumvent this barrier by using allotopic expression which is defined as a wild-type version of defective mitochondrion-encoded gene is delivered *via* a suitable vector to the nucleus of recipient cells. The corresponding mRNA is translated in the cytosol and the protein imported into the mitochondrion, where it should complement the genetic defect. However, because of the highly hydrophobic nature of mitochondrion-encoded proteins,[12] several teams were unable of fully rescuing respiratory chain dysfunction in cultured cells with mtDNA mutations;[13–16] despite some reports described satisfactory results.[17,18] We did benefit from the knowledge, in *Saccharomyces cerevisiae*, on mitochondrial biogenesis and proteome.[19] Reports on electron microscopy described the presence in the mitochondrial outer membrane of specifically attached 80S ribosomes.[20] Biochemical purifications of these ribosomes confirmed that they contained mRNAs encoding mitochondrial proteins.[21] Moreover, biochemical studies established that about 60% of the overall mRNA population encoding mitochondrial proteins specifically localized to the mitochondrial surface[22] and that *cis*-acting elements in the 5′ and 3′ of these genes are involved in this specific localization.[23] Hence, to optimize allotopic expression and guaranty the mitochondrial protein uptake, we built vectors in which the mtDNA sequences were combined with the Mitochondrial Targeting Sequence (MTS) in 5′ and

[1]INSERM, U968, Paris, France; [2]Sorbonne Universités, UPMC Univ Paris 06, UMR_S 968, Institut de la, Vision, Paris, France; [3]CNRS, UMR_7210, Paris, France; [4]Current address: INSERM UMR 1141, Bâtiment Ecran, Hôpital Robert Debré, 48 Boulevard Serurier, Paris, France. Correspondence: M Corral-Debrinski (marisol.corral@inserm.fr)
Received 1 October 2014; accepted 9 January 2015

the 3′UTR (UnTranslated Region) of the nuclear *COX10* gene. *COX10* mRNA, encoding an inner mitochondrial membrane protein involved in heme biosynthesis, is enriched at the surface of the mitochondria in human cells.[24] Consequently the hybrid mRNA should localize to the mitochondrial surface where the translation and the transport are tightly coupled.[25,26] The beneficial effect of the procedure was demonstrated by the rescue of respiratory chain dysfunction in fibroblasts harboring mutations in *ATP6*, *ND1*, or *ND4* genes.[27,28] The extent of complex I or V activity restoration was higher when the *COX10*-3′UTR was used in the constructions instead of the poly adenylation signal of SV40; this is why we consider the procedure as "optimized" relative to the absence of this 3′UTR signal.[27] Next, mitochondrial function modulation through optimized allotopic expression was confirmed *in vivo* since a rat model of ND4 dysfunction in RGCs was generated by electroporation (ELP) of mutant *ND4*.[29] We report here data from experiments conducted in three complementary axes aimed at translating this procedure to the clinic: (i) wild-type human *ND4* expression driven by an adeno-associated virus type 2 (AAV2/2) vector does not cause rat retinal injury, though the lifetime of gene expression was up to 12 months; (ii) human ND4 protein produced from the vector is assembled in CI; (iii) human ND4 protein is able to prevent CI deficiency and optic atrophy in a LHON rat model.

RESULTS

Optimized allotopic expression of the human wild-type *ND4* gene leads to sustained mRNA and protein accumulation in rat retinas without adverse effects on retinal integrity or function

A recombinant AAV2/2 vector harboring the human open reading frame of the mitochondrial *ND4* gene and the signals allowing the efficient mitochondrial translocation of the protein (MTS and 3′UTR of the *COX10* gene) was obtained (AAV2/2-*ND4*) (Figure 1a). It has been reported the long-term ocular gene transfer without adverse effects in mammals (mouse, rat, dog, nonhuman primates) when AAV2 vectors were used.[30] In addition, the serotype 2 is highly efficient on transducing inner retina, primarily RGCs.[31] The question arises whether AAV2/2-*ND4* administration in the vitreous body of rat eyes is able to efficiently transduce RGCs without compromising retinal function. AAV2/2-*ND4* vector was administrated by a single injection in the vitreous body of adult rat eyes at different doses (Supplementary Table S1; Supplementary Material)). First, we evaluated the transduction efficacy by determining the number of RGCs which expressed the GFP (gene included in the vector) in retinal sections from rats euthanized up to 12 months after vector administration. A recent report concluded that BRN3A antibody staining of radial retinal sections is a preferred method for estimating RGC frequency when compared to techniques using retinal whole mounts in rodent models of ocular disease.[32]

When nine independent retinas subjected to AAV2/2-*ND4* administration *via* intravitreal injection were evaluated 6 months postinjection, we found that about 75% of RGCs expressed the transgene indicating both efficient and stable transduction with AAV2/2-*ND4* (Supplementary Figure S1). Next, to determine the kinetics of human *ND4* mRNA appearance, semiquantitative real-time PCR of reverse-transcribed mRNAs (RT-qPCR) were performed with RNAs purified from retinas isolated from eyes subjected to vector administration or contralateral untreated eyes (animals were euthanized between 2 to 16 weeks postinjection). Messenger RNA steady-state levels of the mitochondrial *ATP6* gene was the most stable in the 60 independent samples evaluated. Therefore, it was chosen to normalize the mRNA species and to estimate their relative abundance. Human *ND4* mRNA was detected 2 weeks after vector administration and its amount remained stable 14 weeks later (Figure 1b). This result may be considered as weak when compared to endogenous *ATP6* mRNA; however the signal obtained by RT-qPCR for each mRNA molecule reflected their level in all the retinal cells (~10 millions) while human *ND4* mRNA accumulated only in transduced RGCs representing ~1% of the overall retinal cell population.[33] The human *ND4* transcript was 15.5-fold (Figure 1c) and 331-fold less abundant than *BRN3A* and *SNCG* mRNAs respectively which encode known RGC markers.[34,35] The sustained expression of human *ND4* did not modify the relative abundance of the two transcripts (Figure 1d); indeed mRNA levels in treated eyes relative to untreated ones were not significantly different (*P* values: 0.26 for *BNR3A* and 0.88 for *SNCG*). Protein extractions from single retinas were subjected to Western blotting analyses to determine the steady-state levels of the human ND4 protein in retinas from four treated eyes (6 months after treatment), and compared with the abundance of two CI subunits (NDUFA9 and NDUFB8) and one complex V subunit (ATP synthase α). The antibody against HA1 epitope (three HA1 epitopes are appended at the C-terminal of the human ND4 protein) revealed a signal with an apparent molecular mass of ~54 kDa only in retinas from treated eyes (Figure 1e); the predicted size of the human ND4 protein, after the cleavage of the COX10 MTS, is about 54 kDa: 51.7 kDa for the 459 amino acids of ND4 + ~2.7 kDa for the 27 amino acids of the 3 HA1 epitopes. The mitochondrial proteins NDUFA9, NDUFB8 and ATP synthase α were detected as single bands of approximately 39, 19, and 60 kDa (Figure 1e).

To establish whether human *ND4* expression could be detrimental for retinal function or morphology two parameters were evaluated: eye fundus using confocal Scanning Laser Ophthalmoscopy (cSLO)[36] and optomotor head-tracking responses.[37] SLO evaluations allow obtaining images of the nerve fiber layer in which the disposition of the nerve bundles in a single plane is well resolved because of their cylindrical shape over the pigmented background, thus distinguishing individual bundles of RGC axons becomes possible.[36,38] Evaluations were performed in both eyes from 60 animals subjected to intravitreal administration of AAV2/2-*ND4* (Supplementary Table S1) at four points' postinjection (1, 3, 6, and 9 months). Representative examples of two of animals injected with 10^9 or 10^{10} VG in their left eyes are shown in Figure 2a. Images obtained 3 and 6 months postinjection did not show any difference of nerve fiber densities, when compared to those of eyes before vector administration, indicating that wild-type *ND4* expression did not lead to noticeable RGC axon disappearance. Next, optomotor head-tracking responses were recorded in 30 rats 6 months after AAV2/2-*ND4* administration and in 24-week-old control rats (Figure 2b). Three grating frequencies were tested in clockwise and counterclockwise directions of motion and responses scored for left eyes and right eyes respectively were similar for all of them; thus we illustrated those of the 0.25 cycle per degree frequency (Figure 2b). Control rats mostly presented head tracking responses of similar magnitude for the clockwise (LE) or counterclockwise (RE) drum rotations ($P = 0.58$). Scores recorded in rats subjected to AAV2/2-*ND4* administration were similar to control rat responses ($P = 0.76$ and 0.79 for clockwise motion and 10^9 and 10^{10} VG respectively). Therefore, long-term human *ND4* expression did not lead to deleterious effects on optic fiber densities or visual function.

Human ND4 protein localizes to rat RGC mitochondria and interacts with respiratory chain complex I proteins

The subcellular distribution of the human ND4 protein was examined by immunohistochemistry using antibodies against BRN3A

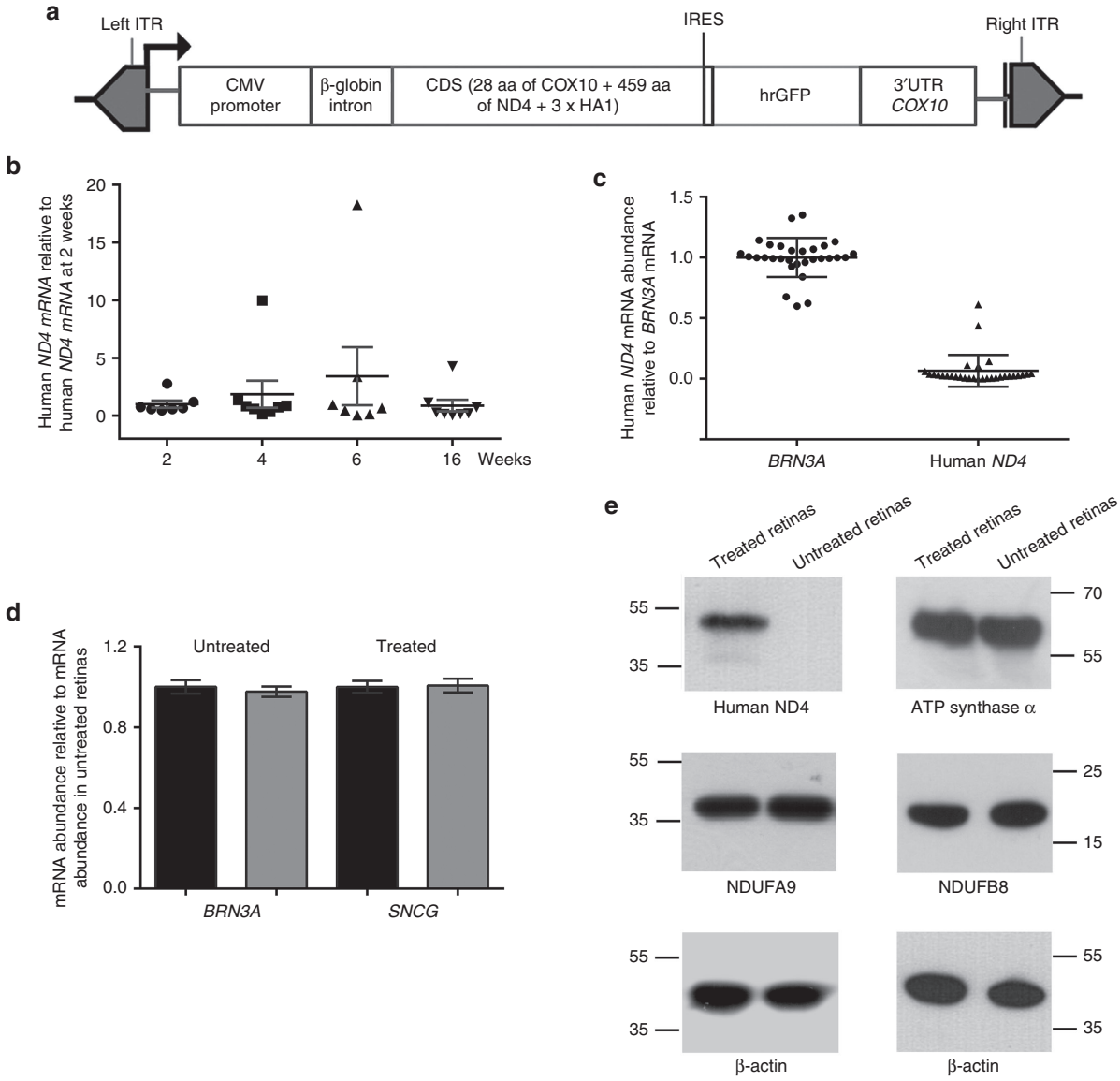

Figure 1 AAV2/2-*ND4* transduction of rat retinas. (**a**) Physical map of the AAV2/2-*ND4* vector genome (7792 bp), encompassing human ND4 sequence inserted into the pAAV-IRES-hrGFP plasmid: the ND4 ORF (1377 bp), encoding 459 amino acids (YP_003024035.1), is in frame at the N-terminal with the first 28 amino acids (84 bp) of human COX10 and C-terminal with three HA1 epitopes (90 bp) and transcribed under the control of the Cytomegalovirus (CMV) promoter and the β-globin intron. The construction contains at the 3′ the untranslated region (603 bp) of the human *COX10* mRNA (NM_001303.3). The sequences are flanked by inverted terminal repeats (ITRs) that contain all the cis-acting elements necessary for replication and packaging of the AAV2/2 vector. (**b**) RT-qPCR assays were performed with total RNAs from retinas (isolated at different times after 5×10^9 VG/eye intravitreal injection of AAV2/2-*ND4*) to determine relative abundance of human *ND4* mRNA. The kinetics of the human *ND4* mRNA apparition was determined between 2 and 16 weeks after intravitreal injection; values shown correspond to the normalization of the human *ND4* mRNA signal against the *ATP6* mRNA signal; seven to eight independent RNA preparations per time-post injection were assessed. (**c**) The relative abundance of human *ND4* and *BRN3A* mRNAs was compared in treated eyes which implies the normalization of *BRN3A* and human *ND4* signals with the mean of the signals obtained for the *BRN3A* mRNA (30 independent results were represented). (**d**) *BRN3A* and *SNCG* mRNA abundances were evaluated in 30 treated eyes relative to their contralateral untreated eyes; values were normalized against means obtained in the untreated eyes per mRNA evaluated. No significant difference was evidenced between treated and untreated retinas; P values were 0.58 and 0.89 for *BRN3A* and *SNCG* mRNAs respectively. (**e**) Representative Western blots from retinas of untreated eyes and retinas which eyes were subjected to AAV2/2-*ND4* administration (5×10^9 VG); rats were euthanized 6 months after vector administration. Four independent extractions from treated and untreated retinas were evaluated. Each western blot was performed two to four times, and the following antibodies were sequentially used: anti-HA1, anti-NDUFA9, anti-NDUFB8, anti-ATP synthase α and anti-β-actin. The anti-HA1 antibody revealed a signal of approximate ~54 kDa only in treated retinas which may correspond to the human ND4 protein. The "PageRuler Plus Prestained Protein Ladder" allowed the estimation of apparent molecular mass of each signal; in the margin of each autoradiogram are annotated the recombinant proteins from the ladder with similar electrophoretic properties than the ones revealed in the membrane after Western blotting (proteins spanning 15–70 kDa).

and the HA1 epitope in retinal sections from six rats euthanized 3–6 months after AAV2/2-*ND4* administration. We observed RGC-positive signal for the anti-HA1 antibody; furthermore, the immunoreactivity was often revealed as a punctuate distribution of fluorescent dots excluded from the nuclei which could represent mitochondria (Figure 3a). To confirm the localization of the human ND4 in the mitochondrial compartment, antibodies against the mitochondrial protein ND6 (a CI subunit) and the HA1 epitope were combined (Figure 3b). Several cells within the ganglion cell layer (GCL) were intensely labeled in the cytoplasm, signals appeared

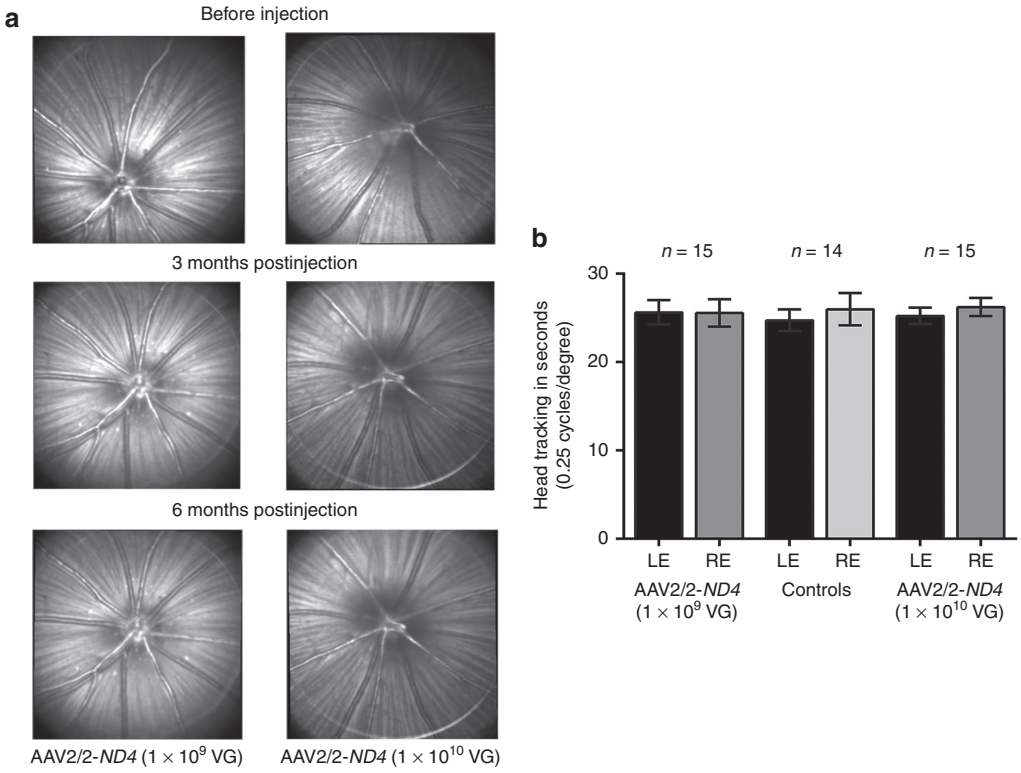

Figure 2 Morphological and functional *in vivo* evaluation of adult rats after ocular administration of AAV2/2-*ND4*. (**a**) Eight-week-old rats were subjected to injection with different doses of the AAV2/2-*ND4* vector (Supplementary Table S1) in the vitreous body of their left eyes. Twelve animals were evaluated for each dose using a cSLO at different points post-injection. Images shown were taken 3 and 6 months after vector administration; eyes before the intervention are also shown (left panel). No change was noticed in nerve fiber density after AAV2/2-*ND4* administration (1×10^9 or 1×10^{10} VG). (**b**) Three different groups of rats were evaluated for head tracking movements in photopic conditions. No significant difference was observed in any of the 30 animals examined in both clockwise (LE) and counterclockwise (RE) directions of motion when the AAV2/2-*ND4* was administrated at two different doses (1×10^9 and 1×10^{10} VG/left eye). Their optomotor behavior was identical to the one elicited in control rats.

as punctuate fluorescent dots excluded from the nuclei with both antibodies indicating some extent of colocalization between the two proteins. In Figure 3b, the merge of the images illustrates yellow-orange pixels corresponding to the regions in which both proteins appear to be apposed (white arrowheads) within the same cells. This suggests that human ND4 proteins synthesized from the AAV2/2-*ND4* vector localize to the mitochondria.

To determine whether the human ND4 protein is assembled in respiratory chain CI, three pairs of independent retinal sections from eyes transduced with AAV2/2-*ND4* and their untreated counterparts were subjected to *in situ* Proximity Ligation Assay (PLA), which was reported as efficient to prove that two proteins are positioned within close proximity (<40 nm) of each other allows visualization of protein interactions in fixed tissues.[39] Moreover, the reliability of the technique for demonstrating protein interactions was proven in rodent retinal sections.[40–42] For the assay, antibodies against proteins which localize to different mitochondrial compartments were used: five inner membrane proteins: OPA1, SDHA1, ND6, NDUFB6, and NDUFS1 and two outer membrane proteins: VDAC and TOMM20. OPA1 is essential for preserving organelle dynamics[43] and was described as interacting with the 70-kDa (FP) subunit of complex II protein, SDHA1.[44] ND6, NDUFB6, and NDUFS1 are CI subunits; CI is a L-shaped complex consisting of two perpendicular arms: a hydrophobic arm which resides in the inner membrane and a hydrophilic peripheral arm which projects into the matrix; ND4, ND6, and NDUFB6 localize to the membrane while NDUFS1 resides in the hydrophilic arm.[45] It clearly appears that ND4-HA1 interacts with ND6 and NDUFS1, since numerous bright red dots suggestive of closely apposed binding of the antibodies were observed; the overall responses for the HA1 antibody were comparable to those obtained for NDUFB6/ND6 and NDUFB6/NDUFS1 antibody combinations (Figure 4a). Fluorescent signals were particularly apparent in the GCL and also in the inner plexiform layer (IPL) which contains RGC dendrites and bipolar cell axons. Very weak signal was detected when anti-NDUFB6 or anti-HA1 antibodies were combined with anti-VDAC or anti-OPA1 antibodies; these results are indicators for a non-existing interaction between: NDUFB6 and VDAC, NDUFB6 and OPA1, ND4-HA1 and VDAC, ND4-HA1 and OPA1. In contrast, abundant fluorescent spots were detected when the assay was performed with anti-OPA1 and anti-SDHA1 antibodies (Figure 4a,b) confirming that these two proteins are located in close proximity *in vivo* as reported in human fibroblasts in which OPA1 was shown to physically interacts with the 70-kDa (FP) subunit of complex II (*i.e.*, SDHA1) when immunoprecipitation experiments were performed.[44] Importantly, when retinal sections from untreated eyes were assessed using the anti-HA1 antibody, no staining was detected supporting the specificity of the signal in retinal sections from treated eyes (Figure 4b). Hence, these data indicate that the human protein ND4 is present in RGC mitochondria and either physically interacts with ND6 and NDUFS1 or the distance between these three proteins is shorter than 40 nm; strongly suggesting the presence of the human ND4 protein within CI.

Subsequently, we performed Blue Native-PolyAcrylamide Gel Electrophoresis (BN-PAGE) which results in the optimal separation of mitochondrial respiratory chain complexes in their native form, thus allowing to demonstrate whether a protein resides within one

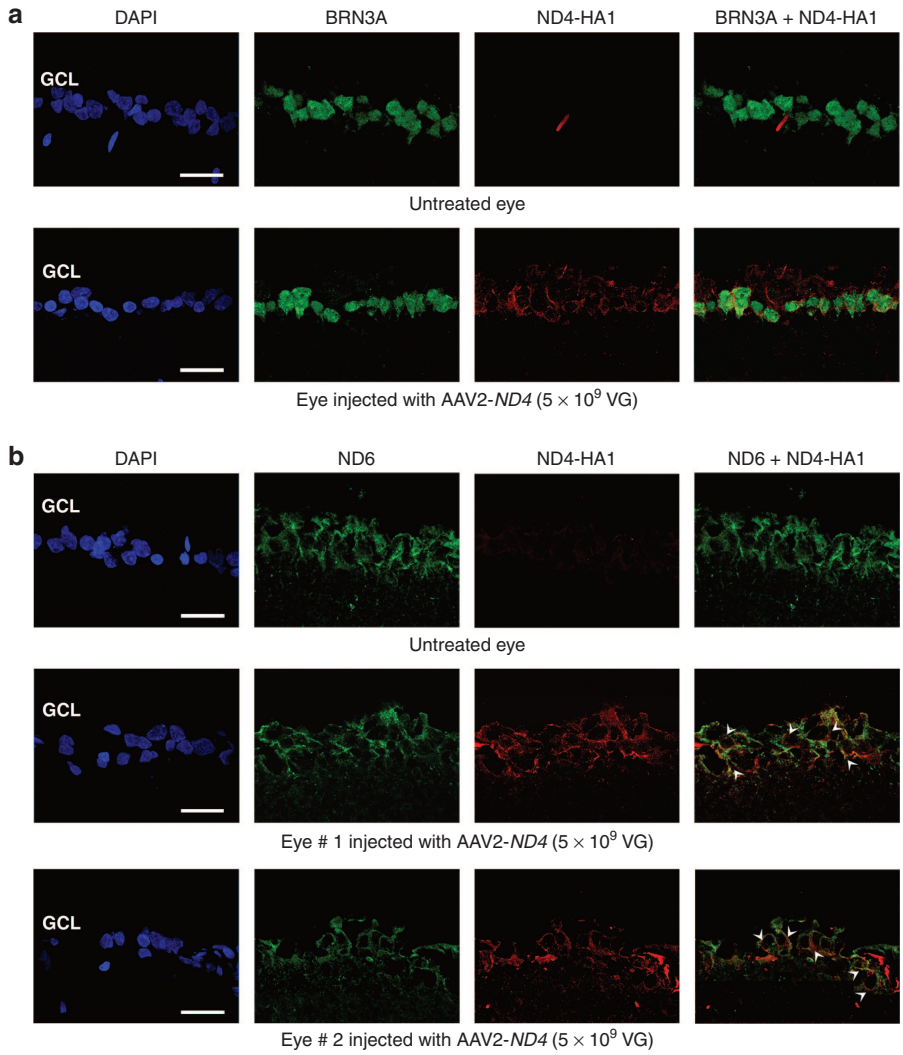

Figure 3 Expression of human ND4 protein in rat retinas. Retinal sections from six independent eyes transduced with AAV2/2-*ND4* (5×10^9 VG/eye) were obtained 3–6 months postinjection. Nuclei were stained with DAPI (blue); GCL represents the ganglion cell layer and scale bars are 20 µm for all panels shown. (**a**) Immunostaining of retinal sections from eyes transduced with AAV2/2-*ND4* (5×10^9 VG/eye) was performed with antibodies against the nuclear factor BRN3A (green) and the HA1 epitope (red); the contralateral untreated eye was used as negative control. (**b**) Retinal sections were double labeled for the mitochondrial ND6 protein (green) and the anti-HA1 epitope (red); images for two treated-eyes and one untreated-eye are illustrated. The yellow-orange pixels (ND6 + ND4-HA1 panel) show that ND6 and ND4-HA1 were in close apposition in some cells (white arrowheads).

of them.[46] Four independent homogenates obtained by combining eight retinas from untreated eyes or eyes transduced with AAV2/2-*ND4* were collected from rats euthanized 3–6 months after vector administration, subjected to two-dimensional blue native/SDS electrophoresis and revealed with specific antibodies against different respiratory chain complex subunits. Figure 5 shows a specific signal when the anti-HA1 antibody was used; the signal was not detected in homogenates from untreated eyes. The specific band evidenced with anti-HA1 antibody migrates slightly slower than NDUFA9 (theoretical molecular mass of 39 kDa) as illustrated (merge between the two autoradiograms, Figure 5, right panel). The putative human ND4 protein migrates similarly to the UQCRC1 subunit of complex III which theoretical molecular mass is ~53 kDa; confirming data obtained with retinal protein extracts (Figure 1e). Indeed, the distance which separates signals from antibodies against NDUFA9 and HA1 epitopes is almost identical than the one which separates signals from antibodies against NDUFA9 and UQCRC1 (Figure 5, bottom panel). Moreover, the anti-HA1 antibody signal was revealed on the same vertical line than NDUFA9, NDUFB8, and NDUFS1. Therefore, the human ND4 protein comigrates with three CI subunits reinforcing the idea that the human ND4 protein is correctly assembled in CI.

Long-lasting expression of the human *ND4* gene in retinas from rats mimicking LHON

The ocular administration of the human *ND4* gene harboring the G11778A mutation *via in vivo* electroporation (ELP) leads to RGC loss, optic atrophy and visual function impairment about 30 days after the intervention in adult rats.[29] To demonstrate that AAV2/2-*ND4* is efficient on preventing RGC dysfunction *in vivo*, we first chose the procedure which better resembles the clinical situation. About 70% of LHON patients bear the G11778A mutation (*ND4* gene) in all the mtDNA molecules of the body.[2] At one moment of patient's life mitochondrial impairment reaches a threshold in which RGCs, unable to ensure their function, degenerate leading to central vision loss.[2,7] In the LHON model we previously described, the coexistence of human ND4 protein with the R340H substitution,

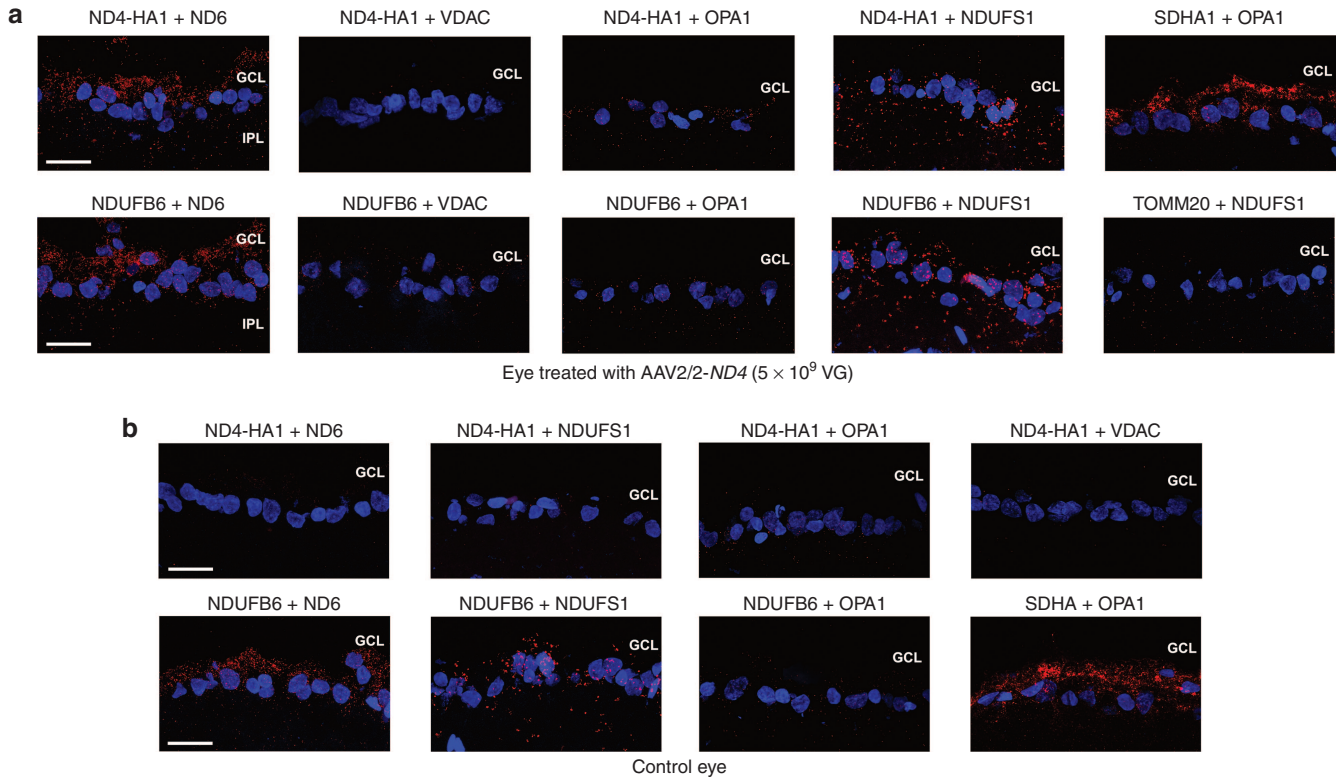

Figure 4 *In situ* PLA analysis of retinal sections from eyes expressing human *ND4*. Retinal sections from three independent eyes treated with AAV2/2-*ND4* or their partner untreated eyes were subjected to *in situ* PLA analysis; the human ND4 protein was revealed using a monoclonal antibody against the HA1 epitope. PLA signals are red and the nuclei stained with DAPI are blue; scale bars correspond to 25 µm. GCL, ganglion cell layer; INL, inner nuclear layer. (**a**) Several combinations of antibodies were tested in retinal sections from eyes subjected to AAV2/2-*ND4* administration. The antibody against HA1 epitope (ND4-HA1) gave strong positive signals when combined with antibodies against ND6 and NDUFS1. No interaction between ND4-HA1 with VDAC or OPA1 protein was inferred by the assay while a strong signal was noticed when antibodies against OPA1 and SDHA1 (70-kDa subunit of complex II) were combined. (**b**) Retinal sections from the untreated eyes were also subjected to the assay. Very weak fluorescence was noticed when the anti-HA1 antibody was used confirming that in treated eyes, signal evidenced corresponded to the human ND4 protein. For all other antibody combinations the results were similar to those obtained in treated eyes.

encoded by the nuclear version of the human *ND4* gene carrying the G11778A mutation, and the endogenous ND4 protein did not engender deleterious effects on RGCs within the first 14 days after *in vivo* ELP.[29] Therefore, 8-week-old rats were subjected to ELP with mutant *ND4* and ten days later, a single intravitreal injection in the electroporated eye was performed with AAV2/2-*ND4* or AAV2/2-*GFP*. Evidently, AAV2/2-*GFP* administration is not expected to counteract the mutant *ND4* effect, neither to induce *in vivo* toxicity.[47] This protocol should allow to seek after AAV2/2-*ND4* ability to protect RGCs: when vector is administrated, mutant *ND4* expression driven by ELP was already started[29] and human *ND4* mRNA accumulates in transduced RGCs about 2 weeks after vector administration (Figure 1b). First, we determined the AAV2/2 transduction efficiency when performed after ELP compared to a single AAV2/2 injection. The overall number of RGCs which were immunolabeled for the GFP in five independent retinal sections was 74.4%; hence, the efficacy of RGC transduction by AAV2/2-*ND4* did not change when rat eyes were first subjected to ELP (Supplementary Figure S1). The presence of human *ND4* mRNA in retinas from treated eyes was determined by RT-qPCR. Animals were euthanized 10–12 months after vector administration and RNA preparations from retinas of 15 untreated eyes and 15 eyes subjected to ELP with mutant *ND4* and intravitreal injection of AAV2/2-*ND4* (10^9 VG or 10^{10} VG) were examined. Human *ND4* mRNA was exclusively detected in treated eyes; its relative amount in these retinas was comparable to the one measured in retinas isolated 4 months after a single AAV2/2-*ND4* intravitreal injection, Figure 1b ($P = 0.21$), confirming a sustained transgene expression overtime (Figure 6a). Besides, human *ND4* mRNA abundance relative to *BRN3A* was about 15-fold lower (Figure 6b) as shown after a single intravitreal AAV2/2-*ND4* injection (Figure 1c). Next, RNA preparations from retinas of 12 eyes transduced with mutant *ND4 via* ELP and subjected 10 days later to an intravitreal injection of AAV2/2-*GFP* were evaluated. A 15% reduction in *SNCG* and *BRN3A* mRNA steady-state levels was measured when RNA preparations from untreated and treated retinas were compared (Figure 6c; $P = 0.0011$ and 0.0003 respectively). This diminution reveals AAV2/2-*GFP* inability to counteract the deleterious effect of mutant *ND4* expression on RGC integrity. Conversely, the relative abundance of *BRN3A* and *SNCG* mRNAs was not significantly different between untreated eyes and eyes from the LHON model expressing the human *ND4* gene; P values were 0.54 and 0.7 respectively (Figure 6d). Therefore, AAV2/2-*ND4* administration hindered RGC loss induced by mutant *ND4* expression.

Effect of AAV2/2-*ND4* treatment on RGC and optic fiber integrity in the LHON model

Eye fundus was performed using cSLO to follow optic fiber integrity in treated eyes. Representative examples are shown in Figure 7a; the eye electroporated with mutant *ND4* and 10 days later transduced with AAV2/2-*GFP* shows a severe loss of optic fibers which corresponds to almost half of the examined area (Figure 7a).

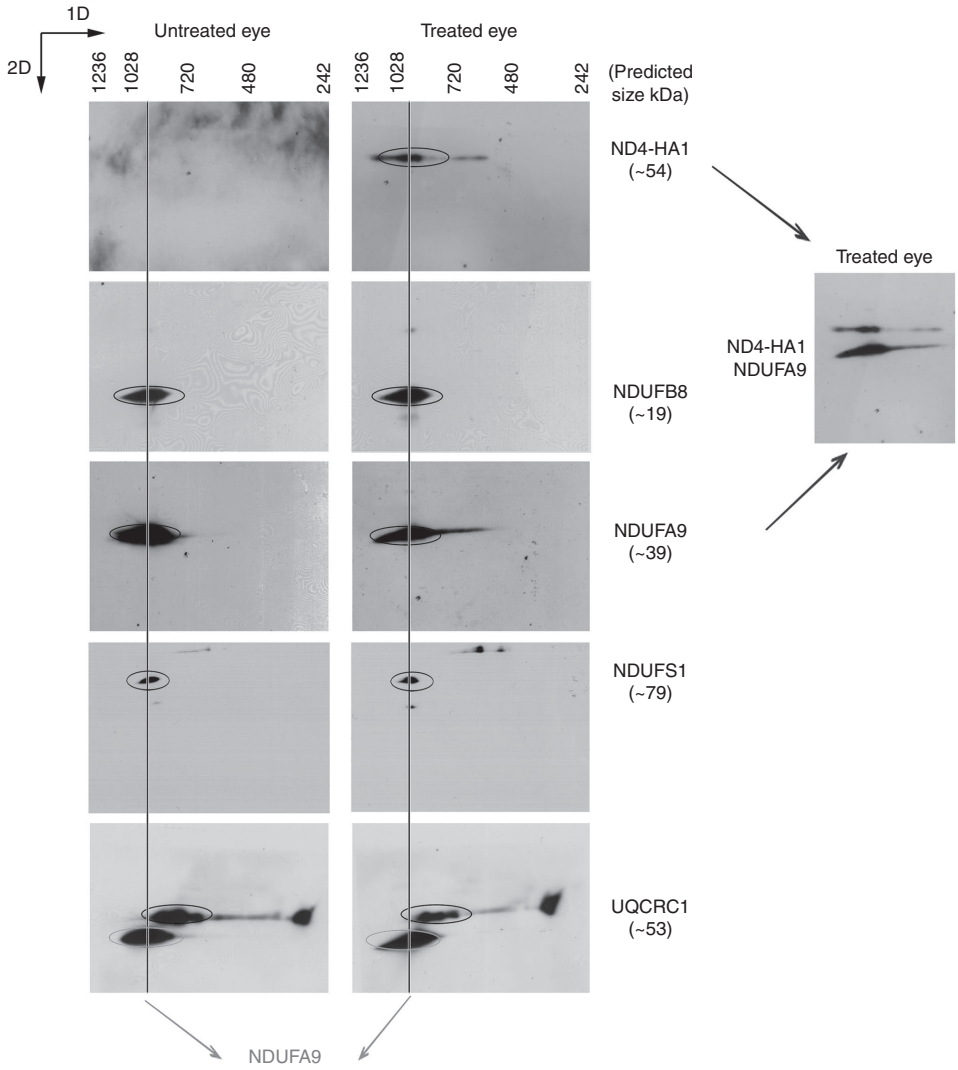

Figure 5 Blue native polyacrylamide gel electrophoresis. Four homogenates (eight pooled retinas) from untreated-eyes or eyes subjected to a single intravitreal injection with AAV2/2-*ND4* were tested with different antibodies (Supplementary Table S2). 2D BN-PAGE of the mitochondrial enriched fractions were subjected to western blotting with antibodies against NDUFA9, NDUFB8 and NDUFS1 proteins of CI, UQCRC1 (CIII) and the HA1 epitope. In the right the superposition of autoradiograms obtained after anti-HA1 and anti-NDUFA9 antibody incubation and in the bottom the superposition for anti-NDUFA9 and anti-UQCRC1 autoradiograms.

The disappearance was generally noticed about 6 weeks after ELP; two times post-AAV2/2 injection are illustrated (3 and 6 months). Out of the 18 eyes evaluated in this group, significant reduction in optic fiber density was evidenced in 6 eyes; by contrast, no RGC axons loss was observed in 52/54 of the animal eyes which were injected with different doses of AAV2/2-*ND4* (Supplementary Table S1). The imaging of one of those animals eye fundus showed that the tracks of RGC axons were well preserved 3 and 6 months after vector administration (Figure 7a). To further confirm these results transversal optic nerves (ONs) sections from the two animals shown in Figure 7a, euthanized 6 months after vector administration, were subjected to immunohistochemistry for the heavy chain subunit of neurofilaments (NF200) to detect RGC axonal profiles. Figure 7b illustrates a recognizable reduction of immunopositive dots in the ON from the animal in which the eye was treated with mutant *ND4* and AAV2/2-*GFP* relative to one ON isolated from an age-matched control rat or to the ON from the rat illustrated in Figure 7a in which the eye was treated with mutant *ND4* and AAV2/2-*ND4*. Since RGC axon number was diminished in eyes electroporated with mutant *ND*4 and treated with AAV2/2-*GFP*, we next estimated RGC number in retinal flat mounts immunostained for BRN3A. Figure 7c shows retinas from untreated eyes and eyes transduced with mutant *ND4* and subsequently treated with AAV2/2-*GFP* or AAV2/2-*ND4*. Mean RGC count per mm^2 ± SEM for 26 retinal flat mounts isolated from untreated eyes was 1796 ± 26.8. These values are similar to those previously described.[33] In contrast, average RGC densities for eight eyes expressing mutant *ND*4 and subjected to AAV2/2-*GFP* injection was 1213 ± 35.7 (Figure 7d); a 33% reduction relative to control retinas. RGC count difference between these two groups was significant ($P < 0.0001$). Conversely, when retinas from eyes expressing mutant *ND4* and transduced with AAV2/2-*ND4* were evaluated a significant protection of the overall RGC density was observed (Figure 7d). The mean of RGC counts per mm^2 was 1741 ± 51.8 (97% of the control value), this number was not significantly different to the one measured in control retinas ($P = 0.24$). Hence, RGC degeneration due to mutant *ND4* expression protein is efficiently prevented by AAV2/2-*ND4* administration.

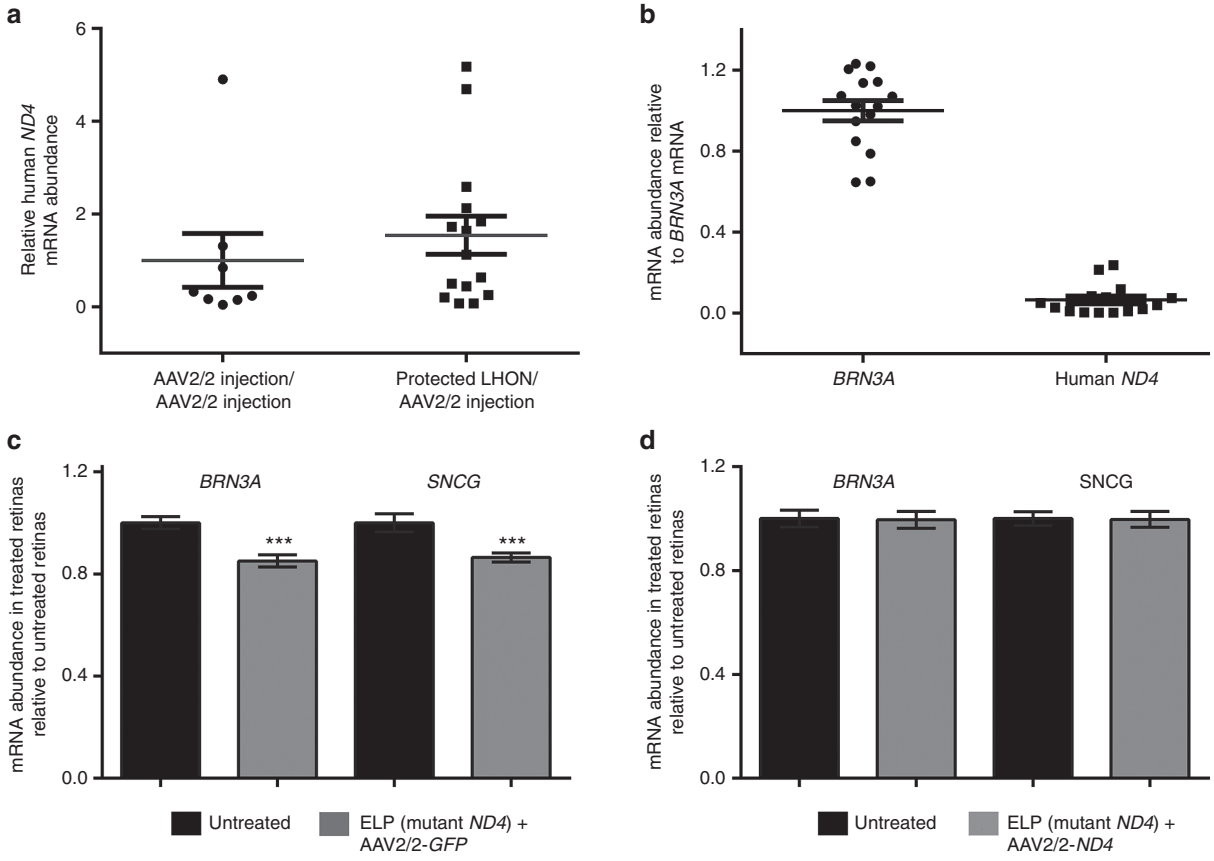

Figure 6 Sustained expression of the human *ND4* gene in the LHON model. RT-qPCRs were performed with: (i) 15 eyes subjected to mutant *ND4* transduction, *via* ELP, and 10 days later to AAV2/2-*ND4* administration; (ii) 12 eyes subjected to mutant *ND4* transduction *via* ELP and 10 days later to AAV2/2-*GFP* administration. As controls, all the contralateral untreated-eyes were evaluated; animals were euthanized between 8 and 12 months after vector administration. (**a**) Human *ND4* mRNA relative abundance in: (i) eight retinas from eyes subjected to a single AAV2/2-*ND4* injection in the vitreous body (rats were euthanized 4 months later) and (ii) 15 retinas from eyes subjected to mutant *ND4* transduction, *via* ELP, and 10 days later to AAV2/2-*ND4* intravitreal injection. (**b**) mRNA abundance relative to *BRN3A* mRNA abundance in 15 RNA preparations from retinas which eyes which received AAV2/2-*ND4* by intravitreal injection 10 days after mutant *ND4* transduction. (**c** and **d**) *BRN3A* and *SNCG* mRNA amounts were compared in RNA preparations from the LHON model: ELP (mutant *ND4*) + AAV2/2-*GFP* or the LHON model in which protection was investigated: ELP (mutant *ND4*) + AAV2/2-*ND4*. Transcript abundance variations are represented relative to the means of values assessed in RNAs from untreated retinas.

Impairment of visual function in the LHON model is prevented by AAV2/2-*ND4* treatment

To examine the impact of human *ND4* expression in the LHON rat model at the functional level, we performed head-tracking experiments to discriminate sensitivities of right eyes or left eyes in the LHON model. We evaluated rats transduced with mutant *ND4* in their left eyes and 10 days later subjected to a single intravitreal injection, in the same eye, with AAV2/2-*GFP* or AAV2/2-*ND4*. Optomotor responses of these groups were compared to head tracking scores for the left or right eyes of 24-week-old control rats (Figure 2). Left eye scores were significantly reduced in animals treated with AAV2/2-*GFP* (40% of right eye responses); they were statistically different to responses recorded for the left eyes in control rats ($P < 0.0001$) indicating that visual performance of eyes expressing mutant *ND4* was compromised. On the other hand, animals which received AAV2/2-*ND4* mostly presented head tracking scores of similar magnitude for each of their eyes ($P = 0.4$). The scores recorded for the left eyes, in the 30 rats evaluated, were similar to control rats ($P = 0.8$). Hence, the salutary impact of AAV2/2-*ND4* administration on nerve fiber integrity (Figure 7a,b) was confirmed by the sustained visual function protection evidenced in the AAV2/2-*ND4* treated eyes.

Respiratory chain complex I activity was preserved in optic nerves from LHON rats when eyes were treated with AAV2/2-*ND4*

To demonstrate that "optimized allotopic expression" of *ND4* is efficient *in vivo* besides the strong indication on the presence of the human ND4 protein within CI (Figures 4 and 5), it is also required setting a robust and reliable assay for CI enzymatic activity. We exploit a spectrophotometric method which allows the sequential evaluation of the enzymatic activities of CI (NADH decylubiquinone reductase) and CV (ATP hydrolase) on a single rodent ON.[48] The sequential evaluation of CI and CV enzymatic activities allowed also CI/CV ratio determination; an accurate parameter for detecting an impairment of respiratory chain activity.[49] Animals were euthanized between 8 and 12 months after AAV2/2 injection. CI and CV activities were assessed in four groups: (i) 84 ONs from untreated eyes; (ii) 30 ONs from eyes subjected to a single AAV2/2-*ND4* intravitreal injection; (iii) 12 ONs from animals injected with AAV2/2-*GFP* (3×10^9 VG) after mutant *ND4* transduction *via* ELP; (iv) 26 ONs from animals injected with AAV2/2-*ND4* after mutant *ND4* transduction *via* ELP. CV activity did not change in any of the groups evaluated when compared to values assessed in control ONs (Figure 8b). The long-term expression of human wild-type *ND4* gene driven by a single AAV2/2

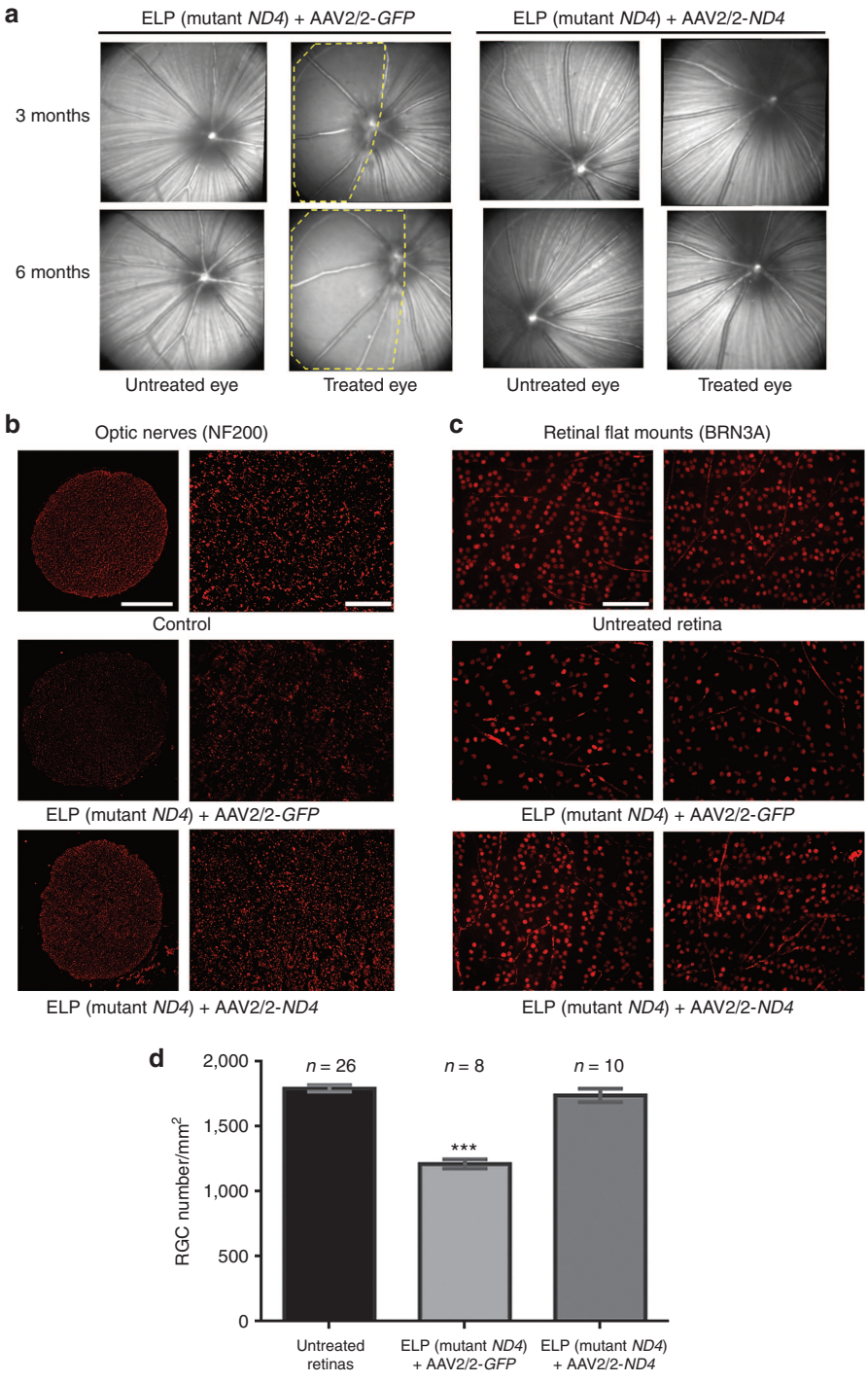

Figure 7 Effect of AAV2/2-*ND4* on RGC and optic fiber integrity in the LHON model. (**a**) cSLO fundus imaging of two rat eyes: one subjected to ELP (mutant *ND4*) + AAV2/2-*GFP* (3×10^9 VG, left panel) and one subjected to ELP (mutant *ND4*) + AAV2/2-*ND4* (5×10^9 VG, right panel) as well as the partner untreated-eyes. Images were taken 3 and 6 months after vector administration; yellow discontinued lines show the region with nerve fiber loss in the eye treated with AAV2/2-*GFP*. (**b**) Proximal ON transversal sections were immunostained with an antibody against NF200 (red); they were obtained from: four rats subjected to intravitreal injection with mutant *ND4*-DNA followed by ELP and 10 days later to another intravitreal injection with AAV2/2-*GFP* (3×10^9 VG) in the same eye; four rats subjected to intravitreal injection with mutant *ND4*-DNA followed by ELP and 10 days later to another intravitreal injection with AAV2/2-*ND4* (5×10^9 VG in the same eye) and four age-matched controls. Images shown correspond to ONs from the two animals from which eye fundus imaging were illustrated in panel **a**. Two different magnifications are shown; scale bars represent 200 µm (left panel) and 25 µm (right panel). The reduction in optic fiber density was evidenced in all the four ON sections evaluated out of the six animals in which eye fundus imaging revealed optic fiber loss. In the contrary, the four ON sections evaluated from eyes treated with AAV2/2-*ND4* gave results similar to those observed in ONs from age-matched controls. (**c**) Retinal flat mounts obtained from animals sacrificed 6 months after vector administration were immunolabeled for BRN3A antibody (red). Images of two distinct retinal regions are illustrated for: (i) an untreated retina; (ii) an eye subjected to ELP (mutant *ND4*) + AAV2/2-*GFP*, and (iii) an eye subjected to ELP (mutant *ND4*) + AAV2/2-*ND4*; the scale bar corresponds to 25 µm. (**d**) Histogram shows the means of RGC number/mm^2 ± SEM obtained after all the BRN3A-positive cells were counted in the three groups evaluated.

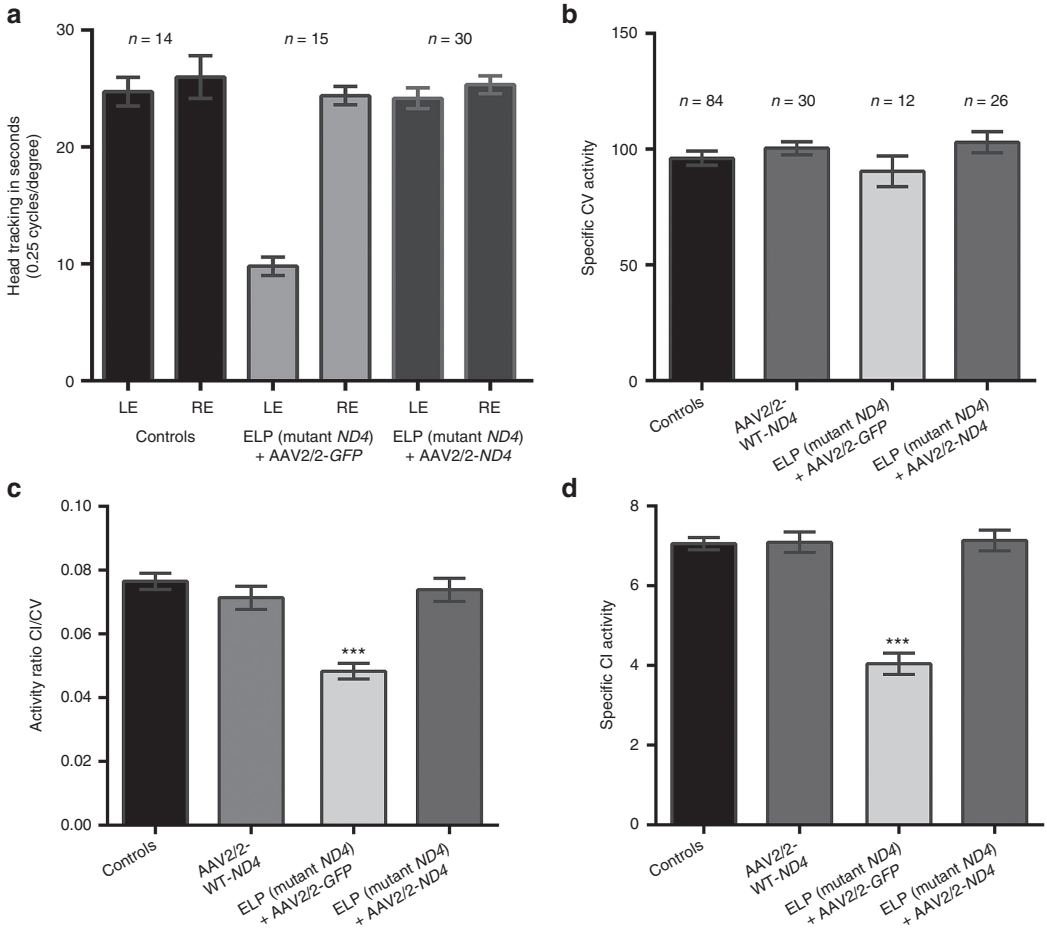

Figure 8 Assessment of visual function and complex I activity in LHON rats. (**a**) Visual behavior was evaluated with the optomotor test in four groups of animals: (i) 14 control rats (24 weeks of age); (ii) 15 animals transduced with mutant *ND4*-DNA *via* ELP + AAV2/2-*GFP* (3×10^9 VG); (iii) 15 animals transduced with mutant *ND4*-DNA *via* ELP + AAV2/2-*ND4* (5×10^8 VG); (iv) 24 animals transduced with AAV2/2-mutant *ND4* (5×10^9 VG). Values presented are expressed as the mean of head tracking per minute (in seconds) ± SEM for each group (spatial frequency of 0.25 cycle per degree). Animals were subjected to the test 6 and 9 months after vector administration. Results obtained for groups 3 and 4 were almost identical, therefore, they were combined and illustrated as a single group ($n = 30$). Respiratory chain CI and CV activities were assessed by spectrophotometry in single ONs, from animals euthanized 8–12 months after intravitreal injection, ONs were isolated from: (i) 84 untreated eyes (controls); (ii) 30 eyes subjected to intravitreal injection with the AAV2/2 harboring the wild-type *ND4* gene (AAV2/2-WT-*ND4*), two doses evaluated (5×10^8 VG and 5×10^9 VG) gave similar results, and are illustrated as a single group; (iii) 12 eyes subjected to mutant *ND4* transduction *via* ELP + AAV2/2-*GFP* (negative control); and (iv) 26 eyes subjected to mutant *ND4* transduction *via* ELP + AAV2/2-*ND4*, two doses evaluated (5×10^8 VG and 5×10^9 VG) gave similar results, and are illustrated as a single group. Respiratory chain CI and CV activities are expressed as nanomoles of oxidized NADH/min/mg protein. (**b**) CV activity measurements were shown, no difference was observed between ONs from treated eyes relative to controls; *P* values for groups 2–5 were respectively: 0.17, 0.94, 0.46, and 0.18. (**c** and **d**) Histograms representing the CI/CV activity ratios and specific CI in the samples evaluated clearly confirm the reduction of CI activity in ONs from eyes subjected to mutant *ND4* transduction; the reduction was efficiently prevented by AAV2/2-*ND4* administration. CI - CV, complexes I and V of the respiratory chain; CI/CV, activity ratio of CI for CV; each enzymatic activity was measured in triplicates and illustrated as means ± SEM.

intravitreal injection was safe for CI function (Figure 8c,d); since no significant difference was observed when CI or CI/CV values were compared to those measured in control ONs (*P* value was 0.92 or 0.25 respectively). On the contrary, mutant *ND4* expression led to CI defect in ONs from eyes treated with AAV2/2-*GFP* after *in vivo* ELP with mutant *ND4* (Figure 8c,d); the reduction of about 40% relative to untreated eyes was significant ($P < 0.0001$ for either specific CI activity or CI/CV ratio). Furthermore, AAV2/2-*ND4* was efficient on protecting CI function; indeed CI activity or CI/CV ratios was not statistically different from values obtained in ONs from untreated eyes: *P* values were 0.7 and 0.98 respectively (Figure 8c,d). Thus, at the molecular level the human ND4 protein largely hindered the deleterious effect of mutant *ND4* expression by preserving CI activity.

DISCUSSION

The first evidence that mitochondrial impairment yields to human disease was described in 1962.[50] In 1988, it was demonstrated that mtDNA deletions were present in the muscle of people suffering from mitochondrial myopathy,[51] and that a mtDNA mutation was responsible for LHON.[52] Up to date molecular defects observed in both mtDNA-encoded and nuclear DNA-encoded genes of mitochondrial proteins are associated with a wide spectrum of clinical problems[8,53] including myopathy, encephalomyopathy, gastrointestinal syndromes, dystonia, diabetes, blindness, deafness, and cardiomyopathy. Therefore, mitochondrial disorders represent a common cause of chronic morbidity and are more prevalent than previously thought; indeed they affect at least 1 in 5,000 individuals.[54] Nevertheless, mitochondrial medicine only made slow

progress towards effective treatment of these devastating diseases; a recent review encompassing 1,335 reports and 12 randomized controlled treatment trials in mitochondrial diseases, did not find a clear evidence supporting the efficacy of any of these interventions.[55] Hence, our main objective was to develop a gene therapy that could prevent optic atrophy due to mitochondrial dysfunction. In this pursuit, we have focused our interest on the LHON disease due to the G11778A mutation on the mitochondrial *ND4* gene, since its accounts for 60-90% of LHON cases worldwide[2] with less than 20% chance of recovery.[7] Clinical manifestations in LHON patients are very peculiar; indeed about 75% of them present sequential visual loss in each eye, with the interval between the first and second eye involvement ranging from weeks to 2–4 months.[7] This opportunity along with the evidence that gene therapy is well tolerated and efficient in Leber Congenital Aumorosis[56] has great potential for a generalization to mitochondrial disorders specially devastating neurodegenerative diseases.[53]

However, an array of obstacles needs to be overcome before being able to offer a clinical protocol safe and beneficial to patients harboring mtDNA mutations. The greatest difficulties are: (i) the scarcity of reliable experimental models of the disease required for the validation of gene therapy or pharmacological approaches *in vivo*. In this respect, a report of Dr. Wallace and colleagues is very promising since it describes the generation of a mouse model with the G13997A mutation in the *ND6* gene, leading to an amino acid substitution (P25L), reported in an optic atrophy and Leigh syndrome family[57]; the mice exhibit some of the LHON hallmarks, especially optic atrophy;[58] (ii) inserting genetic material directly into mtDNA is up to date a difficult task; the reports of J. Guy and colleagues in which the modification of an AAV vector leads to the expression of the transgene inside the mitochondria could allow progress in this pathway[10,11]; (iii) the efficacy of allotopic expression *in vivo* is still under debate. Several reports since 2002 provided controversial results *in vitro*, in which authors indicated that mitochondria behavior in cultured cells can give a false impression on allotopic expression achievement.[14–16] For instance, Perales-Clemente's *et al*.[15] claimed a potential generalization of their data on unsuccessful allotopic expression, because in a mouse cell line, in which wild-type mtDNA was <10%, respiratory chain dysfunction rescue was due to the artefactual selection of revertants from the mutated gene. However authors did not prove this statement; indeed these cells when transduced with any kind of vector should be equally able to drive CI assembly. Moreover, independent groups worldwide did show unambiguously that allotopic expression results on the functionality of the protein within the mitochondria in mice and rats,[29,59–63] and in cancer cells.[64] Additionally, it was reported the generation of transgenic mice for wild-type or a mutated version of the mitochondrial *ATP6* gene *via* allotopic expression. The approach was successful in the mitochondrial delivery of ATP6 derived from the nuclear transcripts. Besides, transgenic mice expressing the mutated gene (single nucleotide change equivalent to the human mutation responsible for Neuropathy, Ataxia and Retinitis Pigmentosa) displayed performance inferior to control mice in four out of seven neuromuscular and motor assays. Though the characterization and comparison of the two transgenic mice should be completed, these experiments reinforce the notion that allotopic expression is efficient *in vivo*.[65]

Therefore, our aim was to make the undeniable proof-of-principle that: (i) *in vivo* allotopic expression of human *ND4* leads to the efficient mitochondrial import and assembly of the protein in CI without affecting its activity; (ii) its expression, driven by an AAV2 vector, impedes vision loss in a LHON rat model by fully preventing CI defect due to mutant *ND4* expression. We first demonstrated that the human ND4 protein, which shares 67% of identity and 84% of similarity with the rat protein, can efficiently compete with this latter and assemble into a functional rat CI by using two independent protocols: (i) The PLA assay[39] corroborated *in situ* interaction of human ND4 with ND6 or NDUFS1, two CI proteins. (ii) BN-PAGE experiments[46] showed that human ND4 (molecular mass of ~54 kDa) migrated similarly than NDUFA9, NDUFB8, and NDUFS1, three subunits of CI indicating its presence within assembled CI. Importantly, human *ND4* expression driven by AAV2/2 was sustained for up to 12 months in about 75% of the total RGC population with no change in cell viability or function. This was supported by: (i) eye fundus imaging; (ii) optomotor behavior, (iii) RGC number estimation; (iv) CI activity assessment in ONs.

The next step was to confirm the effectiveness of AAV2/2-*ND4* treatment in a reliable animal model of LHON. It is well known that in some mtDNA diseases, not all mtDNA molecules are affected and the extent of heteroplasmy is accountable of symptom severity.[66] In LHON patients, the *ND4* mutation is generally homoplasmic but some rare cases of heteroplasmy were described; for instance in a clinically unaffected member from the fifth generation of an Australian pedigree[67] and in pedigrees of the G11778A LHON mutation from Thailand in which the proportion of mutated mtDNA correlated with visual loss.[68] Hence to better mimic what happens in LHON patients and permit the use of AAV2/2-*ND4* to assess its ability to impede RGC loss we designed an improved protocol of eye intervention different to the one we previously reported:[29] an intravitreal injection of a plasmid carrying mutant *ND4* followed by *in vivo* ELP and 10 days later the same eye was subjected to an intravitreal injection of either AAV2/2-*ND4* or AAV2/2-*GFP*. Then, it becomes feasible to compare the effect of *GFP* or human *ND4* protein accumulation in eyes that express mutant *ND4*. The benefit of AAV2/2-*ND4* for RGC integrity was proven by the fact that the ~33% RGC number reduction in eyes expressing mutant *ND4* was prevented in eyes subjected to AAV2/2-*ND4* injection. This data was in agreement with eyes fundus visualizations and ON immunostaining for NF200 which clearly showed that nerve fiber preservation was only noticed when rat eyes were treated with AAV2/2-*ND4*. As expected, rats in which eyes possessed optic fiber density comparable to controls responded normally to the optomotor test. In contrast, animals transduced with *GFP* consistently showed an approximate 40% reduction in their treated eye scores. Unquestionably, the final demonstration of AAV2/2-*ND4* effectiveness on protection against the deleterious effect of mutant *ND4* and hence on the achievement of *in vivo* allotopic expression is provided by the spectrophotometric measurement of CI enzymatic activity in ONs. CI and CV activities were measured in ONs from control animals and values obtained were reliable since only minor fluctuations were noticed. Consequently, CI activity diminution measured in ONs from eyes that expressed mutant *ND4* reflects compromised mitochondrial function in remaining RGC axons. Assessments of CI activity in ONs from eyes subjected to AAV2/2-*ND4* administration undeniably showed the preservation of CI function. Even though we did not circumvent the lack of a genuine genetic model for LHON, we demonstrated that mutant *ND4* injury in the model used for testing AAV2/2-*ND4* effect was identical to the one evidenced previously using *in viv*o ELP.[29] This emphasizes the authenticity of mutant *ND4* detrimental effect on RGC viability. Accordingly, the benefit of human wild-type ND4 protein in the LHON model was reinforced because the protein was capable to protect RGC function durably and safely.

In conclusion, we provide converging lines of evidence that optimized allotopic expression is safe and efficient *in vivo*, therefore, the clinical trial for LHON patients bearing the G11778A mutation using AAV2/2-*ND4* was initiated (NCT02064569). The follow-up of enrolled subjects will have a strong accent on evaluating safety (lack of adverse events related to vector injection) but it can also begin to address the potential for benefit in terms of visual function. Clinically meaningful improvement including patient's quality of life will depend on RGC functional plasticity.[69] Hypothetically, residual RGCs in treated LHON patients could optimize their connectivity leading to structural and functional reorganization close to the macula. This region is responsible for color and high acuity vision due to the largest concentration of cones. A putative rewiring inside the retina may work in concert with a cortical plasticity in the visual cortex, recently described in asymptomatic LHON carriers.[70] At last, if the clinical trial is safe and efficacious, the strategy could be extended to other devastating neurodegenerative disorders with mitochondrial etiology from which few efficient treatments are available up to date.[55]

MATERIALS AND METHODS

Adeno-associated viral vectors

The vector used for gene therapy is a recombinant AAV2/2 containing the human NADH dehydrogenase 4 (*ND4*) gene under the control of the cytomegalovirus immediate early promoter in an intron-containing expression cassette (β globin intron, HBB2), flanked by the viral inverted terminal repeats of the pAAV-IRES-hrGFP vector (Agilent Technologies, Les Ulis, France). The human open reading frame (ORF) of *ND4* was recoded for the 34 non universal codons and optimized to achieve high-level expression in mammalian cells; in frame with the AUG codon was appended 84 base pairs encoding the first 28 amino acids of COX10 corresponding to the mitochondrial targeting sequence (MTS). The human growth hormone polyA signal originally included in the vector (478 nucleotides) was replaced by 603 nucleotides of the human *COX10* 3′ UTR; instead of the full-length 3′UTR previously described.[29] Indeed, pAAV-IRES-hrGFP can only accommodate inserts ≤1.7 kb. The vector leads to the synthesis of the human ND4 protein in which three HA1 epitopes are appended at its C-terminal immediately followed by two stop codons; the whole ORF was synthesized by GenScript. As negative control, the pAAV-IRES-hrGFP was used without ORF but the GFP. The AAV2/2-*ND4* was manufactured either in the Vector Core of Genethon (http://www.genethon.fr/en/); its titer was 1.6×10^{12} VG/ml or the "Centre de Production de Vecteurs and the INSERM UMR1089, Nantes" which titer was 1.6×10^{11} VG/ml. AAV2/2-*GFP* and AAV2/2-mutant *ND4* vectors, also obtained from Nantes, had titers of 6.2×10^{11} VG/ml and 8.3×10^{11} VG/ml respectively.

Animals

Male Long Evans rats were used at 8-week old (Janvier, Le Genest Saint Isle, France); they were housed two per cage in a temperature-controlled environment and 12 hour light/dark cycle. All animal studies were conducted in accordance with the guidelines issued by the French Ministry of Agriculture and the Veterinarian Department of Paris (Permit number DF/DF_2010_PA1000298), the French Ministry of Research (Approval number 5575) and UPMC/INSERM ethics committees (Authorization number 75–1710).

In vivo electroporation and intravitreal injection of AAV2/2 vectors

The ELP procedure was performed in one eye as previously described.[29] After dilatation of the pupil with topical 1% tropicamide (CibaVision) and under anesthesia with isoflurane (40 mg/kg body weight), the protocol was initiated with the injection in the vitreous body of 20 µg (5 µl) of pAAV-IRES-hrGFP plasmid containing the human *ND4* gene harboring the G11778A mutation and 3 Flag epitopes appended to the last amino acid codon. Next, contact-lens-type and needle electrodes were positioned, and square wave pulses were delivered by a Square Wave Electroporation System (ECM 830; BTX, Harvard Apparatus, Les Ulis, France) as previously described.[29] For AAV2/2 administration, intravitreal injections were performed with 5 µl of vector suspension using an ophthalmic surgical microscope. Supplementary Table S1 recapitulates the eyes subjected to AAV2/2 administration, vectors, and the doses used.

Fundus imaging by confocal scanning laser ophthalmoscopy (cSLO)

The Heidelberg Retina Angiograph (Heidelberg Engineering, Dossenheim, Germany) is a scanning laser ophthalmoscope (cSLO) which allows imaging of eye fundus. To adapt the commercial system to the optics of rodent eyes, the 40 mm focal lens of the front objective was replaced by a 25 mm focal lens (Linos Optics, Milford, MA). The system allows the examination of nerve fiber layer in each cardinal area of rat eyes before treatment and different times after vector administration. Images were obtained using the 30° field of view and the automatic real-time mode at a sensitivity setting that maximized the signal/noise ratio; all the cardinal areas of the eye fundus were observed, thus, obtaining fiber bundle distribution in the whole retina. The built-in software was used for postprocessing the images, including alignment, adjustment of contrast, construction of a mean image and/or of a composite image, as previously described.[36]

Optomotor tests

The head-tracking method is based on an optomotor test frequently used in rodents.[29,37] The protocol yields independent measures of right and left eye acuities based on their unequal sensitivities to pattern rotation: right and left eyes are most sensitive to counterclockwise and clockwise rotations, respectively.[37] Long Evans rats were placed individually on an elevated horizontal platform surrounded by a motorized drum (12°/s) in photopic conditions. Vertical black-and-white lines of three varying widths, subtending 0.125, 0.25, and 0.5 cycle/degree (cyc/deg) were presented to the animal and rotated alternatively clockwise and counterclockwise, each for 60 seconds. Head movements were recorded with a video camera mounted above the apparatus; light levels were kept at 240 lux. Animals were scored only when the speed of the head turn corresponded to the rotation speed of the stripes. Assessments were performed before ocular treatment and monthly after the ocular intervention; experimenters were blind to previously recorded results, and thresholds were regularly confirmed by more than one observer.

Retinal and optic nerve histology

Retinas or optic nerves were fixed in PBS + 4% paraformaldehyde at 4 °C and then cryoprotected by overnight incubation in PBS containing 30% sucrose at 4 °C. Retinas were embedded in optimal cutting temperature compound (Neg 50, Richard-Allan Scientific, Villebon-Sur-Yvette, France) and frozen in liquid nitrogen. Optic nerves were embedded in a solution of PBS + 7.5% gelatin from porcine skin Type A (Sigma-Aldrich, Saint-Quentin Fallavier, France) and 10% sucrose and frozen in a 2-methyl-butane solution at −45 °C. Ten micrometer-thick cryosections of retinas and optic nerves were cut on a cryostat (Microm HM550, ThermoScientific, Villebon-Sur-Yvette, France). For immunochemistry, retinal sections were rinsed with PBS and treated for 10 minutes with PBS + 0.1% Triton and then for 1 hour with 1% BSA, 0.1% Triton, and 0.05% Tween 20. Next, they were incubated with primary antibody overnight at 4 °C. Sections were washed in PBS and incubated with appropriate secondary antibodies and DAPI (Sigma-Aldrich) for 2 hours at room temperature. Primary and secondary antibodies used are shown in Supplementary Table S2. For retinal flat mounts, the protocol previously described was followed.[8]

In situ proximity ligation assay

Duolink Kit (Olink Bioscience, Uppsala, Sweden) is based on in situ PLA, proximity ligation assay technology which allows visualization of protein interactions in fixed tissues.[39] In the assay, oligonucleotide-tagged secondary antibodies are linked with circle-forming oligonucleotides. If two antigens, detected by primary antibodies derived from different species, are in close proximity (<40 nm) to each other, after the ligation step of the two linker oligonucleotides, the rolling circle amplification using complementary fluorophore-tagged oligonucleotide probes results in fluorescent puncta at the site of interaction. The technique has been reported as effective demonstrating protein interactions in rodent retinal sections.[41,42] Assays were performed with retinal sections from 4 independent eyes treated with AAV2/2-ND4 (5×10^9 VG) obtained 3–6 months postinjection or their fellow untreated eyes. The manufacturer's instructions were essentially followed using the different antibodies listed in Supplementary Table S2. Briefly, different mouse antibodies against: HA1 epitope, NDUFB6 (complex I subunit), SDHA1 (the 70-kDa (FP) subunit of complex II) or TOMM20 (mitochondrial translocase of the outer membrane) in combination with rabbit antibodies against: ND6 (complex I subunit), NDUFS1 (complex I subunit), VDAC (outer mitochondrial membrane protein), or OPA1 (inner mitochondrial membrane) were used.

Microscopic observations

Fluorescence labeling was monitored at the Cellular Imaging Facility of the Vision Institute with a confocal laser scanning microscope FV1000 (Olympus) and a fluorescence microscope (Leica DM5000 B). Image acquisition was conducted with Olympus Fluoview software version 3.1 and the the MetaVue software. Finally, all the images were analyzed with Photoshop and Image J softwares.

RNA extraction and RT-qPCR assay

Total RNA from rat retinas were extracted using RNeasy Plus Mini kit from Qiagen (Courtaboeuf, France). To ensure the absence of DNA, a treatment with RNase-free DNase (Qiagen) and a subsequent cleanup with the RNeasy MinElute cleanup kit (Qiagen) were performed. This was confirmed by subjecting 10 ng of each RNA preparation to qPCR with human *ND4,* endogenous *ATP6* or *BRN3A* primers. One microgram of total RNA was reverse transcribed with oligo-dT using Superscript II Reverse Transcriptase (Life Technologies, Saint-Aubin, France). Quantitative PCR reactions were performed using ABI 7500 Fast (Applied Biosystems, Saint Aubin, France) and the specific primers (Life Technologies) listed in Supplementary Table S3. The equivalent of 10 and 2 ng of cDNAs were used per gene as template for qPCR reactions with Power Sybr green PCR Master Mix (Applied Biosystems). Each biological sample was subjected to the assay in triplicates per gene; Ct values (number of cycles required for the fluorescent signal to cross the background threshold) were obtained with the ABI 7500 software (v.2.0.4). To determine the relative mRNA amount of each studied gene we used the comparative $\Delta\Delta C_t$ method and the mitochondrial *ATP6* gene as normalizing gene since its mRNA steady-state levels remained almost unchanged in all the samples evaluated.

Western blotting analysis and blue native polyacrylamide gel electrophoresis

For whole proteins extracts, single retinas were homogenized in 50 µl of 20 mmol/l HEPES and 60 mmol/l mannitol (pH 7.2) using a 200 µl micro-hand-driven glass–glass potter at 4 °C. Large cellular debris was spun down by a low speed centrifugation (1,000 *g* for 5 minutes at 4 °C) and supernatants were subjected to protein quantification (Bradford reagent). Fifteen and 30 µg of protein extracts from: four control retinas and four retinas which received AAV2/-*ND4* intravitreally were denaturated at 94 °C for 15 minutes, resolved in 12% SDS-PAGE and transferred to a PVDF membrane. Membranes were probed with antibodies against HA1 epitope, NDUFA9, NDUFB8, ATP synthase subunit α and β-actin (Supplementary Table S2). Immunoreactive bands were visualized with appropriate secondary antibodies coupled to horseradish peroxidase (0.1 mg/ml) (Supplementary Table S2) followed by detection with Pierce ECL Plus Western Blotting Substrate (Pierce, ThermoScientific, Villebon-Sur-Yvette, France). Apparent molecular mass of each protein was estimated by comparing the electrophoretic properties of each specific signal in the immunoblots with the "PageRuler Plus Prestained Protein Ladder" (Pierce Protein Biology products, ThermoScientific).

For blue native polyacrylamide gel electrophoresis (BN-PAGE) mitoplasts isolation was adapted from the report of Calvaruso *et al.*[46] Briefly, after careful dissection, retinas were kept frozen and samples were prepared at ice-melting temperature by homogenization of 8 retinas using a 1 ml hand-driven glass–glass potter in 1 ml of ACBT buffer (aminocaproic acid 1.5 mol/l; Bis-Tris 75 mmol/l; pH 7). 100 µl of β-lauryl-maltoside 20% (Biorad, Marnes-la-Coquette, France) were added to allow the isolation of respiratory chain complexes. The mixture was kept on ice for 10 minutes and then centrifuged for 30 minutes at 14,000 rpm. The protein content of the supernatant was measured with the BCA protein assay kit (Pierce ThermoScientific) and then kept at −20 °C until use. BN-PAGE 5–15% gradient gels were casted and then loaded with 200 µg of proteins. To perform two-dimensional blue native/SDS electrophoresis, lanes were cut out of the first dimension and incubated with 1% SDS and 1% β-mercaptoethanol for one hour at room temperature. The gel strip was placed at the top of glass plates in order to poor the SDS gel (4% for stacking and 10% for separation). Next, standard western blotting protocols for SDS gels were applied.[46] Immunodetection was performed using primary antibodies against proteins of the respiratory chain (Supplementary Table S2). To reuse membranes, the antibody was removed with the Re-Blot Plus Western Blot Strong Antibody Stripping Solution (Millipore, Molsheim, France).

Tissue homogenate preparation and respiratory chain enzyme assays

Optic nerves were rapidly collected and kept frozen (−80 °C). CI and CV activities were measured using a Cary 50 UV-Vis spectrophotometer (Agilent Technologies) as described for retinas and ONs from rodents.[48] CI activity values were either normalized by CV or converted to specific activities (expressed as nanomoles of oxidized NADH/minute/mg protein) after protein quantification by the Bradford method. All chemicals were of the highest grade from Sigma-Aldrich.

Statistical analyses

Values are expressed as means ± standard error of the mean. Statistical analyses were performed with the GraphPad Prism 6.0 software assuming a confidence interval of 95%. Data collected for all the independent observations were compared using the non parametric significance test of Mann–Whitney (*≤0.05, **≤0.01, and ***≤0.005).

CONFLICT OF INTEREST

J.-A.S. is one of the cofounders of GenSight Biologics, a privately owned biopharmaceutical company, dedicated to the development and commercialization of gene therapy based treatments of retinal degenerative diseases. The company obtained the patent-licensing arrangement for the clinical development of AAV2/2-*ND4* (GS010). The clinical trial started in February 2014 (NCT02064569). There are no other patents, products in development or marketed products to declare.

ACKNOWLEDGMENTS

We are grateful to Pierre Rustin for useful discussions and comments on the manuscript; to Soufien Sghari (Master degree internship) and Delphine Roussel (engineer) for the realization of RT-qPCR assays in animals subjected to AAV2/2-*ND4* administration. We are especially thankful to Leo G. Nijtmans and Mariël A. M. van den Brand (Nijmegen Centre for Mitochondrial Disorders at the Department of Pediatrics, Radboud University Nijmegen Medical Centre, The Netherlands) who thought us how to perform BN-PAGE experiments. This work was supported by funds from the INSERM and the CNRS (UMR-S 968; UMR 676); Association Française contre les Myopathies (AFM), Agence Nationale pour la Recherche (ANR)/Maladies Rares and Emergence-Bio. Conceived and designed the experiments: H.C.-T. and M.C.-D. Performed the experiments: H.C.-T., S.A., C.L., J.A., and M.C.-D. Analyzed the data: H.C.-T., S.A., C.L., J.A., and M.C.-D. Contributed as head of the Research Center: J.-A.S. Wrote the paper: H.C.-T., S.A., and M.C.-D.

REFERENCES

1. Man, PY, Griffiths, PG, Brown, DT, Howell, N, Turnbull, DM and Chinnery, PF (2003). The epidemiology of Leber hereditary optic neuropathy in the North East of England. *Am J Hum Genet* **72**: 333–339.
2. Yu-Wai-Man, P, Griffiths, PG and Chinnery, PF (2011). Mitochondrial optic neuropathies - disease mechanisms and therapeutic strategies. *Prog Retin Eye Res* **30**: 81–114.
3. Carelli, V, La Morgia, C, Valentino, ML, Barboni, P, Ross-Cisneros, FN and Sadun, AA (2009). Retinal ganglion cell neurodegeneration in mitochondrial inherited disorders. *Biochim Biophys Acta* **1787**: 518–528.
4. Klopstock, T, Yu-Wai-Man, P, Dimitriadis, K, Rouleau, J, Heck, S, Bailie, M *et al.* (2011). A randomized placebo-controlled trial of idebenone in Leber's hereditary optic neuropathy. *Brain* **134**(Pt 9): 2677–2686.
5. Carelli, V, La Morgia, C, Valentino, ML, Rizzo, G, Carbonelli, M, De Negri, AM *et al.* (2011). Idebenone treatment in Leber's hereditary optic neuropathy. *Brain* **134**(Pt 9): e188.
6. Sadun, AA, Chicani, CF, Ross-Cisneros, FN, Barboni, P, Thoolen, M, Shrader, WD *et al.* (2012). Effect of EPI-743 on the clinical course of the mitochondrial disease Leber hereditary optic neuropathy. *Arch Neurol* **69**: 331–338.
7. Newman, NJ (2012). Treatment of hereditary optic neuropathies. *Nat Rev Neurol* **8**: 545–556.
8. Cwerman-Thibault, H, Augustin, S, Ellouze, S, Sahel, JA and Corral-Debrinski, M (2014). Gene therapy for mitochondrial diseases: Leber Hereditary Optic Neuropathy as the first candidate for a clinical trial. *C R Biol* **337**: 193–206.
9. Mileshina, D, Ibrahim, N, Boesch, P, Lightowlers, RN, Dietrich, A and Weber-Lotfi, F (2011). Mitochondrial transfection for studying organellar DNA repair, genome maintenance and aging. *Mech Ageing Dev* **132**: 412–423.
10. Yu, H, Ozdemir, SS, Koilkonda, RD, Chou, TH, Porciatti, V, Chiodo, V *et al.* (2012). Mutant NADH dehydrogenase subunit 4 gene delivery to mitochondria by targeting sequence-modified adeno-associated virus induces visual loss and optic atrophy in mice. *Mol Vis* **18**: 1668–1683.
11. Yu, H, Koilkonda, RD, Chou, TH, Porciatti, V, Ozdemir, SS, Chiodo, V *et al.* (2012). Gene delivery to mitochondria by targeting modified adenoassociated virus suppresses Leber's hereditary optic neuropathy in a mouse model. *Proc Natl Acad Sci USA* **109**: E1238–E1247.
12. Claros, MG, Perea, J, Shu, Y, Samatey, FA, Popot, JL and Jacq, C (1995). Limitations to *in vivo* import of hydrophobic proteins into yeast mitochondria. The case of a cytoplasmically synthesized apocytochrome b. *Eur J Biochem* **228**: 762–771.

13. Oca-Cossio, J, Kenyon, L, Hao, H and Moraes, CT (2003). Limitations of allotopic expression of mitochondrial genes in mammalian cells. *Genetics* **165**: 707–720.
14. Bokori-Brown, M and Holt, IJ (2006). Expression of algal nuclear ATP synthase subunit 6 in human cells results in protein targeting to mitochondria but no assembly into ATP synthase. *Rejuvenation Res* **9**: 455–469.
15. Perales-Clemente, E, Fernández-Silva, P, Acín-Pérez, R, Pérez-Martos, A and Enríquez, JA (2011). Allotopic expression of mitochondrial-encoded genes in mammals: achieved goal, undemonstrated mechanism or impossible task? *Nucleic Acids Res* **39**: 225–234.
16. Figueroa-Martínez, F, Vázquez-Acevedo, M, Cortés-Hernández, P, García-Trejo, JJ, Davidson, E, King, MP *et al.* (2011). What limits the allotopic expression of nucleus-encoded mitochondrial genes? The case of the chimeric Cox3 and Atp6 genes. *Mitochondrion* **11**: 147–154.
17. Guy, J, Qi, X, Pallotti, F, Schon, EA, Manfredi, G, Carelli, V *et al.* (2002). Rescue of a mitochondrial deficiency causing Leber Hereditary Optic Neuropathy. *Ann Neurol* **52**: 534–542.
18. Manfredi, G, Fu, J, Ojaimi, J, Sadlock, JE, Kwong, JQ, Guy, J *et al.* (2002). Rescue of a deficiency in ATP synthesis by transfer of MTATP6, a mitochondrial DNA-encoded gene, to the nucleus. *Nat Genet* **30**: 394–399.
19. Premsler, T, Zahedi, RP, Lewandrowski, U and Sickmann, A (2009). Recent advances in yeast organelle and membrane proteomics. *Proteomics* **9**: 4731–4743.
20. Kellems, RE, Allison, VF and Butow, RA (1975). Cytoplasmic type 80S ribosomes associated with yeast mitochondria. IV. Attachment of ribosomes to the outer membrane of isolated mitochondria. *J Cell Biol* **65**: 1–14.
21. Ades, IZ and Butow, RA (1980). The products of mitochondria-bound cytoplasmic polysomes in yeast. *J Biol Chem* **255**: 9918–9924.
22. Garcia, M, Darzacq, X, Delaveau, T, Jourdren, L, Singer, RH and Jacq, C (2007). Mitochondria-associated yeast mRNAs and the biogenesis of molecular complexes. *Mol Biol Cell* **18**: 362–368.
23. Saint-Georges, Y, Garcia, M, Delaveau, T, Jourdren, L, Le Crom, S, Lemoine, S *et al.* (2008). Yeast mitochondrial biogenesis: a role for the PUF RNA-binding protein Puf3p in mRNA localization. *PLoS One* **3**: e2293.
24. Sylvestre, J, Margeot, A, Jacq, C, Dujardin, G and Corral-Debrinski, M (2003). The role of the 3′ untranslated region in mRNA sorting to the vicinity of mitochondria is conserved from yeast to human cells. *Mol Biol Cell* **14**: 3848–3856.
25. Kaltimbacher, V, Bonnet, C, Lecoeuvre, G, Forster, V, Sahel, JA and Corral-Debrinski, M (2006). mRNA localization to the mitochondrial surface allows the efficient translocation inside the organelle of a nuclear recoded ATP6 protein. *RNA* **12**: 1408–1417.
26. Ahmed, AU and Fisher, PR (2009). Import of nuclear-encoded mitochondrial proteins: a cotranslational perspective. *Int Rev Cell Mol Biol* **273**: 49–68.
27. Bonnet, C, Kaltimbacher, V, Ellouze, S, Augustin, S, Bénit, P, Forster, V *et al.* (2007). Allotopic mRNA localization to the mitochondrial surface rescues respiratory chain defects in fibroblasts harboring mitochondrial DNA mutations affecting complex I or v subunits. *Rejuvenation Res* **10**: 127–144.
28. Bonnet, C, Augustin, S, Ellouze, S, Bénit, P, Bouaita, A, Rustin, P *et al.* (2008). The optimized allotopic expression of ND1 or ND4 genes restores respiratory chain complex I activity in fibroblasts harboring mutations in these genes. *Biochim Biophys Acta* **1783**: 1707–1717.
29. Ellouze, S, Augustin, S, Bouaita, A, Bonnet, C, Simonutti, M, Forster, V *et al.* (2008). Optimized allotopic expression of the human mitochondrial ND4 prevents blindness in a rat model of mitochondrial dysfunction. *Am J Hum Genet* **83**: 373–387.
30. Surace, EM and Auricchio, A (2008). Versatility of AAV vectors for retinal gene transfer. *Vision Res* **48**: 353–359.
31. Hellström, M, Ruitenberg, MJ, Pollett, MA, Ehlert, EM, Twisk, J, Verhaagen, J *et al.* (2009). Cellular tropism and transduction properties of seven adeno-associated viral vector serotypes in adult retina after intravitreal injection. *Gene Ther* **16**: 521–532.
32. Mead, B, Thompson, A, Scheven, BA, Logan, A, Berry, M and Leadbeater, W (2014). Comparative evaluation of methods for estimating retinal ganglion cell loss in retinal sections and wholemounts. *PLoS One* **9**: e110612.
33. Salinas-Navarro, M, Mayor-Torroglosa, S, Jiménez-López, M, Avilés-Trigueros, M, Holmes, TM, Lund, RD *et al.* (2009). A computerized analysis of the entire retinal ganglion cell population and its spatial distribution in adult rats. *Vision Res* **49**: 115–126.
34. Surgucheva, I, Weisman, AD, Goldberg, JL, Shnyra, A and Surguchov, A (2008). Gamma-synuclein as a marker of retinal ganglion cells. *Mol Vis* **14**: 1540–1548.
35. Nadal-Nicolás, FM, Jiménez-López, M, Sobrado-Calvo, P, Nieto-López, L, Cánovas-Martínez, I, Salinas-Navarro, M *et al.* (2009). Brn3a as a marker of retinal ganglion cells: qualitative and quantitative time course studies in naive and optic nerve-injured retinas. *Invest Ophthalmol Vis Sci* **50**: 3860–3868.
36. Paques, M, Simonutti, M, Roux, MJ, Picaud, S, Levavasseur, E, Bellman, C *et al.* (2006). High resolution fundus imaging by confocal scanning laser ophthalmoscopy in the mouse. *Vision Res* **46**: 1336–1345.
37. Douglas, RM, Alam, NM, Silver, BD, McGill, TJ, Tschetter, WW and Prusky, GT (2005). Independent visual threshold measurements in the two eyes of freely moving rats and mice using a virtual-reality optokinetic system. *Vis Neurosci* **22**: 677–684.
38. Kanamori, A, Catrinescu, MM, Traistaru, M, Beaubien, R and Levin, LA (2010). *In vivo* imaging of retinal ganglion cell axons within the nerve fiber layer. *Invest Ophthalmol Vis Sci* **51**: 2011–2018.
39. Söderberg, O, Leuchowius, KJ, Gullberg, M, Jarvius, M, Weibrecht, I, Larsson, LG *et al.* (2008). Characterizing proteins and their interactions in cells and tissues using the in situ proximity ligation assay. *Methods* **45**: 227–232.
40. Venkatesan, JK, Natarajan, S, Schwarz, K, Mayer, SI, Alpadi, K, Magupalli, VG *et al.* (2010). Nicotinamide adenine dinucleotide-dependent binding of the neuronal Ca2+ sensor protein GCAP2 to photoreceptor synaptic ribbons. *J Neurosci* **30**: 6559–6576.
41. Caminos, E, Vaquero, CF and Martinez-Galan, JR (2015). Relationship between rat retinal degeneration and potassium channel KCNQ5 expression. *Exp Eye Res* **131**: 1–11.
42. Lee, A, Wang, S, Williams, B, Hagen, J, Scheetz, TE and Haeseleer, F (2015). Characterization of Cav1.4 Complexes (alpha11.4, beta2, alpha2delta4) in HEK293T cells and in the retina. *J Biol Chem* **290**: 1505–1521.
43. Belenguer, P and Pellegrini, L (2013). The dynamin GTPase OPA1: more than mitochondria? *Biochim Biophys Acta* **1833**: 176–183.
44. Zanna, C, Ghelli, A, Porcelli, AM, Karbowski, M, Youle, RJ, Schimpf, S *et al.* (2008). OPA1 mutations associated with dominant optic atrophy impair oxidative phosphorylation and mitochondrial fusion. *Brain* **131**(Pt 2): 352–367.
45. Vogel, RO, Smeitink, JA and Nijtmans, LG (2007). Human mitochondrial complex I assembly: a dynamic and versatile process. *Biochim Biophys Acta* **1767**: 1215–1227.
46. Calvaruso, MA, Smeitink, J and Nijtmans, L (2008). Electrophoresis techniques to investigate defects in oxidative phosphorylation. *Methods* **46**: 281–287.
47. Schindehütte, J, Fukumitsu, H, Collombat, P, Griesel, G, Brink, C, Baier, PC *et al.* (2005). *In vivo* and *in vitro* tissue-specific expression of green fluorescent protein using the cre-lox system in mouse embryonic stem cells. *Stem Cells* **23**: 10–15.
48. Lechauve, C, Augustin, S, Cwerman-Thibault, H, Reboussin, É, Roussel, D, Lai-Kuen, R *et al.* (2014). Neuroglobin gene therapy prevents optic atrophy and preserves durably visual function in Harlequin mice. *Mol Ther* **22**: 1096–1109.
49. Rustin, P, Chretien, D, Bourgeron, T, Wucher, A, Saudubray, JM, Rotig, A *et al.* (1991). Assessment of the mitochondrial respiratory chain. *Lancet* **338**: 60.
50. Luft, R, Ikkos, D, Palmieri, G, Ernster, L and Afzelius, B (1962). A case of severe hypermetabolism of nonthyroid origin with a defect in the maintenance of mitochondrial respiratory control: a correlated clinical, biochemical, and morphological study. *J Clin Invest* **41**: 1776–1804.
51. Holt, IJ, Harding, AE and Morgan-Hughes, JA (1988). Deletions of muscle mitochondrial DNA in patients with mitochondrial myopathies. *Nature* **331**: 717–719.
52. Wallace, DC, Singh, G, Lott, MT, Hodge, JA, Schurr, TG, Lezza, AM *et al.* (1988). Mitochondrial DNA mutation associated with Leber's hereditary optic neuropathy. *Science* **242**: 1427–1430.
53. McFarland, R, Taylor, RW and Turnbull, DM (2010). A neurological perspective on mitochondrial disease. *Lancet Neurol* **9**: 829–840.
54. Schaefer, AM, McFarland, R, Blakely, EL, He, L, Whittaker, RG, Taylor, RW *et al.* (2008). Prevalence of mitochondrial DNA disease in adults. *Ann Neurol* **63**: 35–39.
55. Pfeffer, G, Majamaa, K, Turnbull, DM, Thorburn, D and Chinnery, PF (2012). Treatment for mitochondrial disorders. *Cochrane Database Syst Rev* **4**: CD004426.
56. Bennett, J, Ashtari, M, Wellman, J, Marshall, KA, Cyckowski, LL, Chung, DC *et al.* (2012). AAV2 gene therapy readministration in three adults with congenital blindness. *Sci Transl Med* **4**: 120ra15.
57. Malfatti, E, Bugiani, M, Invernizzi, F, de Souza, CF, Farina, L, Carrara, F *et al.* (2007). Novel mutations of ND genes in complex I deficiency associated with mitochondrial encephalopathy. *Brain* **130**(Pt 7): 1894–1904.
58. Lin, CS, Sharpley, MS, Fan, W, Waymire, KG, Sadun, AA, Carelli, V *et al.* (2012). Mouse mtDNA mutant model of Leber hereditary optic neuropathy. *Proc Natl Acad Sci USA* **109**: 20065–20070.
59. Qi, X, Sun, L, Lewin, AS, Hauswirth, WW and Guy, J (2007). The mutant human ND4 subunit of complex I induces optic neuropathy in the mouse. *Invest Ophthalmol Vis Sci* **48**: 1–10.
60. Guy, J, Qi, X, Koilkonda, RD, Arguello, T, Chou, TH, Ruggeri, M *et al.* (2009). Efficiency and safety of AAV-mediated gene delivery of the human ND4 complex I subunit in the mouse visual system. *Invest Ophthalmol Vis Sci* **50**: 4205–4214.
61. Chadderton, N, Palfi, A, Millington-Ward, S, Gobbo, O, Overlack, N, Carrigan, M *et al.* (2013). Intravitreal delivery of AAV-NDI1 provides functional benefit in a murine model of Leber hereditary optic neuropathy. *Eur J Hum Genet* **21**: 62–68.
62. Koilkonda, RD, Yu, H, Chou, TH, Feuer, WJ, Ruggeri, M, Porciatti, V *et al.* (2014). Safety and effects of the vector for the Leber hereditary optic neuropathy gene therapy clinical trial. *JAMA Ophthalmol* **132**: 409–420.
63. Koilkonda, R, Yu, H, Talla, V, Porciatti, V, Feuer, WJ, Hauswirth, WW *et al.* (2014). LHON gene therapy vector prevents visual loss and optic neuropathy induced by G11778A mutant mitochondrial DNA: biodistribution and toxicology profile. *Invest Ophthalmol Vis Sci* **55**: 7739–7753.
64. Calabrese, C, Iommarini, L, Kurelac, I, Calvaruso, MA, Capristo, M, Lollini, PL *et al.* (2013). Respiratory complex I is essential to induce a Warburg profile in mitochondria-defective tumor cells. *Cancer Metab* **1**: 11.
65. Dunn, DA and Pinkert, CA (2012). Nuclear expression of a mitochondrial DNA gene: mitochondrial targeting of allotopically expressed mutant ATP6 in transgenic mice. *J Biomed Biotechnol* **2012**: 541245.

66. Nunnari, J and Suomalainen, A (2012). Mitochondria: in sickness and in health. *Cell* **148**: 1145–1159.
67. Sudoyo, H, Marzuki, S, Mastaglia, F and Carroll, W (1992). Molecular genetics of Leber's hereditary optic neuropathy: study of a six-generation family from Western Australia. *J Neurol Sci* **108**: 7–17.
68. Chuenkongkaew, WL, Suphavilai, R, Vaeusorn, L, Phasukkijwatana, N, Lertrit, P and Suktitipat, B (2005). Proportion of 11778 mutant mitochondrial DNA and clinical expression in a thai population with leber hereditary optic neuropathy. *J Neuroophthalmol* **25**: 173–175.
69. Porciatti, V and Ventura, LM (2012). Retinal ganglion cell functional plasticity and optic neuropathy: a comprehensive model. *J Neuroophthalmol* **32**: 354–358.
70. d'Almeida, OC, Mateus, C, Reis, A, Grazina, MM and Castelo-Branco, M (2013). Long term cortical plasticity in visual retinotopic areas in humans with silent retinal ganglion cell loss. *Neuroimage* **81**: 222–230.

Supplementary Information accompanies this paper on the *Molecular Therapy—Methods & Clinical Development* website (http://www.nature.com/mtm)